-34

N72-14782 (NASA-CR-[redacted]) 119902 AN EXPERIMENTAL STUDY OF AXISYMMETRIC MODES IN VARIOUS PROPELLANT TANKS CONTAINING LIQUID Final Report D.D. Kana, et al (Southwest Research Inst.) May 1971 63 p CSCL 13D G3/27

Unclas 11817

(NASA CR OR TMX OR AD NUMBER)

AN EXPERIMENTAL STUDY OF AXISYMMETRIC MODES IN VARIOUS PROPELLANT TANKS CONTAINING LIQUID

by

Daniel D. Kana

Andrew Nagy

FINAL REPORT

Contract No. NAS8-30167

Control No. DCN 1-9-53-20030

SwRI Project No. 02-2583

Prepared for

National Aeronautics and Space Administration

George C. Marshall Space Flight Center

Marshall Space Flight Center, Alabama

May 1971

SOUTHWEST RESEARCH INSTITUTE

SAN ANTONIO HOUSTON

Reproduced by
NATIONAL TECHNICAL
INFORMATION SERVICE
U S Department of Commerce
Springfield VA 22151

SOUTHWEST RESEARCH INSTITUTE
Post Office Drawer 28510, 8500 Culebra Road
San Antonio, Texas 78228

AN EXPERIMENTAL STUDY OF AXISYMMETRIC MODES IN VARIOUS PROPELLANT TANKS CONTAINING LIQUID

by
Daniel D. Kana
Andrew Nagy

FINAL REPORT

Contract No. NAS8-30167
Control No. DCN 1-9-53-20030
SwRI Project No. 02-2583

Prepared for
National Aeronautics and Space Administration
George C. Marshall Space Flight Center
Marshall Space Flight Center, Alabama

May 1971

Approved:

H. Norman Abramson

H. Norman Abramson, Director
Department of Mechanical Sciences

TABLE OF CONTENTS

PRECEDING PAGE BLANK NOT FILMED

LIST OF ILLUSTRATIONS

LIST OF ILLUSTRATIONS (Cont'd.)

LIST OF ILLUSTRATIONS (Cont'd.)

INTRODUCTION

Recent advancements in space technology and the continued occurrence of POGO oscillations in launch vehicles make it very desirable to develop further a more accurate spring-mass model which can be used to analyze the longitudinal dynamics of such systems. The limited experiments which have been performed on some practical shaped tanks verify that much useful information can be obtained by studying simplified models. A basic model for such representation was developed by Glaser[1*]. To determine the validity of this model, it became desirable to provide experimental data on simple, simulated vehicle structural systems for comparison. Some of the results from these experiments were presented in the Interim Report[2] of the present contract. The data provided in this Report are the results obtained from additional configurations which complement the experimental data reported in Reference 2.

---

* Superscript numbers refer to References at the end of text.

DESCRIPTION OF APPARATUS AND PROCEDURES

The experimental procedure utilized in this phase is similar to that used in the first phase of the program. It was desirable to construct simple structural components, basically thin shells of revolution, whose natural frequencies and responses to forced vibration may be compared with results obtained by using theoretical models. Figures 1 and 2 show two of the models used for the current work and are a way to show the difference between the two supporting systems used in the tests.

Figure 1 shows a cylindrical tank, having a hemispherical bulkhead,supported on columns. This was a standard approach for supporting cylindrical tanks with bulkheads, other than flat-rigid, and also for supporting spherical or ellipsoidal tanks at their center flanges. The tank shown in Figure 1 is a thin-walled cylinder which was described in detail in the Interim Report[2] and was designated throughout that report as the "Lower Tank". With the exception that, in the present case, the bulkhead is an aluminum hemispherical bulkhead rather than ellipsoidal bulkhead, the model is identical in every respect to that shown in Figure 32 in the Interim Report[2].

This supporting technique worked satisfactorily for all configurations where tanks with their coupling flanges were mounted on the columns directly, as shown in Figure 1. Despite the fact that the flanges had some effect on the systems, since they were not infinitely stiff as would be desirable, their influences were readily identified during the tests. For example, a problem arose when this column-type system was attempted to be used for supporting spherical tanks at half radius on their lower or upper halves. A 3/4-inch-thick steel ring was installed on top of the columns and was intended to be used for supporting the spherical tank. When the system was excited, it was found that, even though the input was controlled by the acceleration at one point on the mounting ring, the supporting system was not sufficiently rigid for the intended purpose. Bending responses occurred in both the mounting ring and the columns, and the affect of these responses became so strongly coupled with the response of the tank that it was impossible to identify the natural longitudinal modes. As a result, the massive supporting structure used for these configurations was fabricated and is shown in Figure 2.

The structure consists of a cast aluminum, heavy wall cylinder and two end plates which are bolted to this cylinder. Coupling to the electrodynamic shaker was accomplished by the lower end plate, while the upper ring provided the means of supporting the models to be tested. Figure 2 shows the aluminum spherical tank supported at its upper half radius inside of the massive support structure. Windows cut on the supporting cylinder provide access for obtaining bulkhead mode shapes on the models being tested. This massive support structure has dimensions such that it is capable of supporting the "Upper Tank"[2] at its top. This is shown later in Figures 39 and 41.

Model components, namely the Upper and Lower Tanks, Skirt, Plastic Hemispherical Bulkhead, Ellipsoidal Bulkheads, and Flat-Rigid Bulkheads were described in detail in the Interim Report[2] and will not, therefore, be discussed again here.

In addition to the above-mentioned components, three aluminum hemispherical bulkheads were also used in the program. They were fabricated from 6061-0 aluminum sheets by a spinning process, as were the ellipsoidal bulkheads. Flanges, identical to those on the small ellipsoidal bulkheads[2], were provided during the spinning process to assure interchangeability. One of these hemispherical bulkheads, designated as No. 3, was then modified by the addition of an extra flange at its mid-radius. This modification was accomplished by machining a 1/4-inch-thick aluminum ring to the contour of the bulkhead at the desired location and electron-beam welding it into position. The final step in the fabricating process, was subjecting all three bulkheads to heat treatment to obtain a minimum yield strength of 30,000 psi.

The spinning process for fabricating the above-described bulkheads, in essence, consists of stretching the sheet metal to conform to a pre-machined shape which, in this particular instance, is a hemisphere. This process provides a relatively uniform thickness around a given latitude circle, but an unfortunately significant variation in thickness from the outer circle to the bottom center (i. e., along a meridian). The question then arises as to what thickness should be used when theoretical calculations of natural frequencies are made for such bulkheads. An equal-weight average of thickness is the simplest answer. However, some additional consideration should be made before a final judgement can be effected on this matter. In this regard, it was called to our attention that Reference 3 presents a membrane analysis of a spherical shell with liquid. Results are given as a plot of the nondimensional number

$$\Omega = \left(\frac{\rho\omega^2 R^3}{tE}\right)^{1/2}$$

In this parameter, ρ is the density of the contained liquid, ω is the natural frequency of the system, R and t are the radius and thickness, respectively, and E is the modulus of elasticity for the material of the shell. For a depth of $\eta = h/2R = 0.5$, which is the equivalent of a hemispherical shell filled with fluid, the lowest value of the non-dimensional number Ω is given as 1.20. This is the theoretical value obtained for the first natural longitudinal mode and should prove to be close to that procurable by experiments.

Use of the above-given definition for Ω, with values applicable to the present aluminum models of the hemispherical shells, resulted at first in a number equal to 0.966, which is considerably lower than that given above. This value was obtained by using an average wall thickness of 0.027 inch for the bulkhead in question. Upon further reflection, it was realized that all parameters in the expression for Ω were well defined with the exception of the wall thickness, which varies along the meridian of the shell. By substituting the smallest value measured for the wall thickness, a larger value of the frequency parameter, namely $\Omega = 1.10$ was obtained, which is in closer agreement with the referenced article. These results indicate that proper choice of an effective wall thickness is very essential. Therefore, to assist in the selection of an appropriate average wall thickness for use in theoretical calculations, a graph of the measured wall thickness variation for each hemispherical and ellipsoidal bulkhead is presented in Figures 3 and 4, respectively. Some suitable scheme for developing an effective average thickness remains to be determined. However, from the physical nature of the geometry, it is believed that the thickness near the flange probably has the most influence on symmetric vibrational modes, and a straightforward use of that thickness therefore would be appropriate. As a result, the above-given value of $\Omega = 1.10$ is probably a reasonable value for the case described.

Two sizes of ellipsoidal bulkheads were utilized in the tests as indicated by the graphs in Figure 4. The small bulkheads were especially fabricated for use in this program and were designed to fit with the cylindrical components described in the Interim Report[2]. The large bulkheads were made for a previous program; however, since they were a scaled-up version of the small shells, it seemed useful to also utilize these bulkheads to obtain natural frequency data for comparison between the two sizes.

Liquid propellant was simulated by using distilled water in all models, as was done in the first part of the program. A 12.0-inch-diameter, 0.125-inch-thick aluminum cover plate formed a closure for the hemispherical and semi-ellipsoidal tanks. It will be shown later that this plate also added rigidity to the support. Ullage pressure was then provided to preclude the possibility of buckling of the inverted bulkheads or the cylinder supporting the liquid-filled spherical tank and, in all cases, to increase the natural frequencies of nonsymmetric modes above the frequency range of interest. As was noted in the Interim Report[2], ullage pressure had only a negligible effect on the symmetric modes.

Excitation of the models was accomplished with the electrodynamic shaker which was used throughout the preceding phase, and the input was controlled by the accelerometer which is denoted as A_1 on the schematics supplied in this report. These schematics also indicate the additional accelerometers and pressure transducers, where appropriate, and their respective locations on the structures. Amplitudes and relative phase angles between these transducers were employed for determining the natural frequencies of the structures.

EXPERIMENTAL RESULTS

During the first year, attention was concentrated on several model configurations which consisted of one or more cylindrical shells of revolution. These models were outfitted with flat rigid or elastic bulkheads and, in all cases, were supported at their lower-most flanges. Experimental data obtained with these models are presented in Reference 2. During the current work, the following additional configurations were tested:

a) Hemispherical and spherical tanks supported at various points on the tanks

b) Semi-ellipsoidal and ellipsoidal tanks supported at their flanges (which is at the major diameter on the ellipsoidal tank)

c) Cylindrical and spherical tanks in tandem configuration

d) Cylindrical tanks with hemispherical and inverted hemispherical bulkheads supported at their lowest structural points

e) A cylindrical tank with inverted ellipsoidal bulkhead supported at its lowest point

f) A cylindrical tank with flat rigid and elastic bulkhead supported at its top.

Experimental resu_ts obtained on these models, as in the preceding Interim Report[2], are presented by plotting the natural frequencies against liquid depth. The plotted data for each configuration are accompanied by a schematic depicting the model in question which is supplied to facilitate visualization of the model structure for which these data are presented. Geometrical and material property data essential for theoretical calculations are included with the schematics in a tabulated form. In most configurations for which the elastic bulkheads were accessible, mode shapes were noted for each natural frequency and are presented in a sectional line drawing form along with the schematics. They are identified by corresponding mode number on the frequency data.

It should be mentioned here that, as before, results are presented only for those modes which were identified to be axisymmetric about the longitudinal axis. Some bending modes which were excited through eccentricities in the structures were identified in the course of the testing program, but were omitted, since these were not primary linear responses to longitudinal excitation.

Data resulting from experiments conducted on two of the aluminum hemispherical tanks, made from Bulkheads No. 1 and No. 2, are shown in Figures 5 and 6. Natural frequencies for these bulkheads are presented on a common plot to demonstrate their identical responses under similar test conditions. Corresponding bulkhead mode shapes for these frequencies are shown in Figure 5. When counting the flange for one nodal circle and neglecting the nodal circle appearing very close to the flange on the first mode, the number of the nodal circles corresponds to the mode shape numbers. The second nodal circle observed for the first mode probably resulted from bending at the flange and coupling between the shell and the supporting structure. This same behavior was demonstrated by the plastic hemispherical bulkhead for which the experimental results are shown in Figures 7 and 8. Comparison of the data for the aluminum and plastic bulkheads verifies the fact that the elastic properties of the bulkhead will affect the natural frequencies, lowering them in the case of the plastic bulkhead. Pressure profiles along the center lines and meridians of the two aluminum and one plastic hemispherical bulkheads are shown in Figures 9 and 10. It should be pointed out that in order to introduce a pressure transducer into the liquid, the cover plate used during the acquisition of natural frequency data had to be removed. The removal of this plate softened the support systems to some degree, which is indicated by the lower natural frequencies shown in Figures 9 and 10. This effect was quite pronounced for the first mode on the aluminum bulkhead. It must be emphasized again that this was a result of a softened boundary condition, rather than any effects from changed ullage pressure.

For the next step in the program, the No. 1 and No. 2 aluminum hemispherical bulkheads were joined to form a spherical tank supported at its center flange. Two configurations were constructed: Configuration 1, in which bulkhead No. 1 formed the bottom, and Configuration 2, in which bulkhead No. 2 formed the bottom. Natural frequency data along with bulkhead mode shapes for these two conditions are shown in Figures 11-14. General mode shapes for the two configurations are identical, while the natural frequencies deviate from each other to a small degree and only at the liquid levels approaching full condition. If the stiffening effect of the upper half of the tank and the cover plate for the bulkhead were equal (i.e., if the flange boundary conditions were essentially rigid in both cases), then data for the spherical tank at the liquid depth ratio $h/D = 0.5$ should be identical to that for the hemispherical tank filled with liquid. Comparison of the natural frequencies for those two conditions are in close agreement and seem to support the preceding statement.

Results for the small ellipsoidal bulkheads are shown in Figures 15-17, and the natural frequencies for the two bulkheads are again presented on a common frequency versus liquid depth plot. The figure clearly exhibits a difference in natural frequencies for corresponding modes in the two different bulkheads. This frequency difference is the direct result of the thickness difference between the bulkheads as indicated by Figure 4a. The thickness variation is particularly apparent in the near vicinity of the supporting flange and the wall thickness is considerably lower at this location for Bulkhead No. 1. This suggests a decrease in stiffness resulting in a lower frequency level and is in agreement with Figure 16. Pressure profile data presented in Figure 17 are similar to the general mode shapes of the hemispherical bulkheads. The only exception is the second mode along the center line shown in Figure 17a. Examination of Figures 9a, 10a, and 17a seems to indicate that the pressure distribution along the center line is strongly influenced by both the elasticity and geometry of the bulkhead, particularly for higher modes.

Ellipsoidal bulkheads No. 1 and No. 2 were joined to form an ellipsoidal tank for which data are presented in Figures 18 and 19. Again, as it was applied to the spherical tank, a comparison may be drawn between the ellipsoidal bulkhead filled with liquid and the ellipsoidal tank at a liquid depth ratio of $h/d = 0.5$. Frequencies for these conditions are also in good agreement.

Examination of the ellipsoidal tank mode shapes may raise a question concerning the validity of the first and second modes, since they seem to indicate identical conditions. The difference resulted from the fact that while the first mode appeared to either lead or lag the control accelerometer at resonance, the second mode consistently maintained the same phase relationship when resonance was reached.

Results for the large ellipsoidal tank supported at its center flange are shown in Figures 20-23. Natural frequencies of this tank were considerably lower than those for the small tank and became very difficult to identify above 600 Hz when liquid depth in the tank surpassed the mid-level. To help identify the natural frequencies, transfer functions indicating relative pressure response were run for various liquid depths. Representative figures for liquid depth ratios $h/d = 0.329$, 0.5, 0.614, and 0.843 are presented in Figure 23. These figures also very vividly show the change in the amplification ratio with increasing liquid depth in the tank, along with the presence of split modes which most likely would not be predicted by a linear vibration theory.

Figure 24 shows some final data for both the large and small ellipsoidal tanks. The natural frequency parameter described earlier for hemispherical tanks is applied to the ellipsoidal tank data for the first two modes. The correlation appears to be quite good when the thickness is taken as the minimum measured value which occurs near the flanges. These results again seem to indicate that this minimum value is the significant thickness of the tanks.

In the next two configurations, for which data are shown in Figures 25-28, the spherical tank is supported first at its half-radius on the lower hemisphere, and then at its half-radius on its upper hemisphere. Natural frequencies for the latter case are appreciably lower than for the sphere supported on its lower half, which emphasizes the difference in effective stiffness between the two conditions.

The next model is somewhat analogous to the lower tank with flat rigid bulkhead and top mass shown in Figures 3 and 5 in the Interim Report[2]. The difference between these models and the cylinder and sphere tandem configuration shown in Figure 29 of this Report is that, in the present case, the top mass is replaced in part by an effective liquid mass which is frequency dependent. Results for this model are presented in Figures 30a, b, and c, which give the natural frequencies of the structure for varying liquid depths in the cylinder and for fixed liquid depth ratios $h_s/D = 0$, 0.5, and 0.95, respectively, in the sphere. The structural mode appearing at 515 Hz for the empty condition of the sphere is consecutively lowered with increasing liquid depth in the sphere. This mode was identified as the first structural mode for the cylinder. Based on the available data, the structural mode shown at 450 Hz in Figure 30c was judged to be the same mode which is located at 970 Hz for the half-full sphere in Figure 30b; however, it was not strong enough to be observed for the complete liquid level range in the cylinder when the sphere was empty. It should also be pointed out that above 800 Hz the natural modes became increasingly weaker and highly coupled for the case of $h/D = 0.95$ liquid level in the sphere, making identification very difficult.

Results for the cylindrical tank with aluminum hemispherical bulkhead and stiffener rings are given in Figures 31 and 32. Two external modes, namely column and support flange resonances, were detected and are indicated in Figure 32. These modes coupled with the liquid modes of the cylinder, thereby causing some distortion. The expected frequencies of the liquid modes in the absence of these coupling effects are also indicated.

Following this configuration is the model just mentioned with stringers and baffles added onto the cylinder for which the results are shown in Figures 33 and 34. Natural frequencies obtained for the bulkhead alone (data from Figure 6) are indicated on the frequency plot for the model in question. They show very close agreement with the frequencies between liquid levels $h/\ell = -0.379$ and 0 in the cylinder. A comparison could also be attempted between Figures 46 and 47 in the Interim Report[2] and the figures just discussed, to thereby show the combined effect of the rings, stringers, and baffles and a lower bulkhead elasticity on the natural frequencies of the structure.

Data for cylindrical tank with inverted hemispherical and ellipsoidal bulkheads are presented in Figures 35-38. These models show an effect of higher structural stiffness, resulting from the geometrical shape of the bulkheads. That is, corresponding liquid modes are higher in frequency for the ellipsoidal configuration. Also, note that the structural mode occurs near 325 Hz for both cases.

Finally, data for the cylindrical tank, designated in the Interim Report[2] as the upper tank, with flat rigid and hemispherical bulkheads and supported at its top, are presented in Figures 39-42. These data show not only the effect of bulkhead elasticity between the two conditions, but also the change in system response when the structure is supported and excited at its new location as compared to Figures 30 and 31. When supported at its top, the model exhibited a decrease in structural stiffness resulting in lower frequencies, particularly for lower order modes.

It should be emphasized that, for the experimental results throughout this report, curves through the data points have been drawn by best judgement, based on experimental observations, and may require some alterations when compared with results obtained through the use of the theoretical models.

ACKNOWLEDGEMENTS

The authors are most grateful to Messrs. George W. Downey, Jr. and Dennis C. Scheidt for conducting the experimental tests, and to Mr. Victoriano J. Hernandez for preparing the illustrations.

REFERENCES

1. Glaser, R. F., "Longitudinal Mass-Spring Modeling of Launch Vehicles," NASA TN D-537, Washington, D. C., August 1969.

2. Kana, D. D., and Nagy, A., "An Experimental Determination of the Longitudinal Modes of a Simulated Launch Vehicle Dynamic Model," Interim Report, Contract No. DCN 1-9-53-20030, Southwest Research Institute, March 1970.

3. Balabukh, L. I., and Molchanov, A. G., "Axisymmetric Oscillations of a Spherical Shell Partially Filled with Fluid," Inzhenernyi Zhurnal-Mekhanika Tverdogo Tela, Sept.-Oct., 1967, pp. 56-61.

APPENDIX

Illustrations

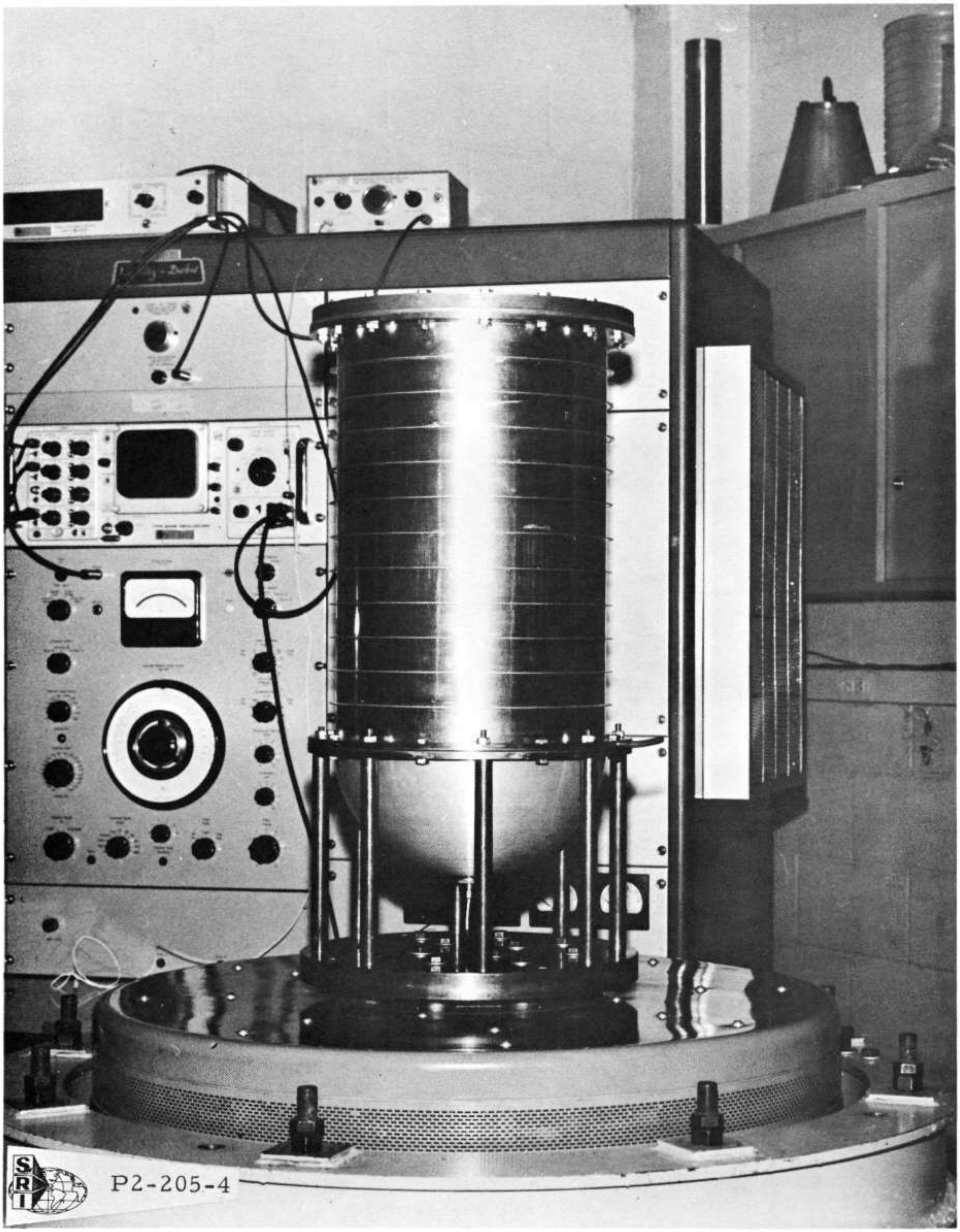

Figure 1. Cylindrical Tank with Hemispherical Bulkhead on Eight-Column Support

NOT REPRODUCIBLE

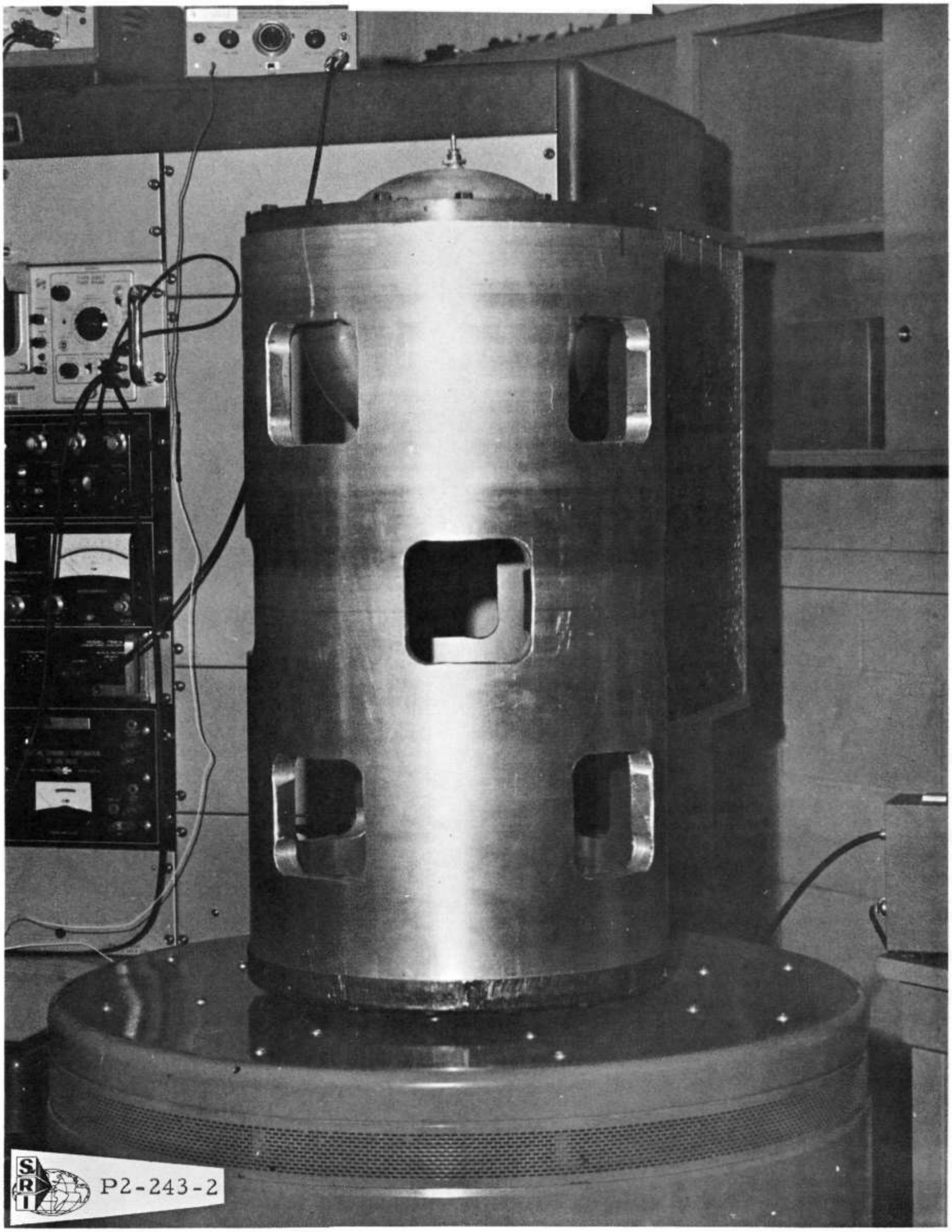

Figure 2. Spherical Tank Mounted at Upper Half-Radius in Massive Support Structure

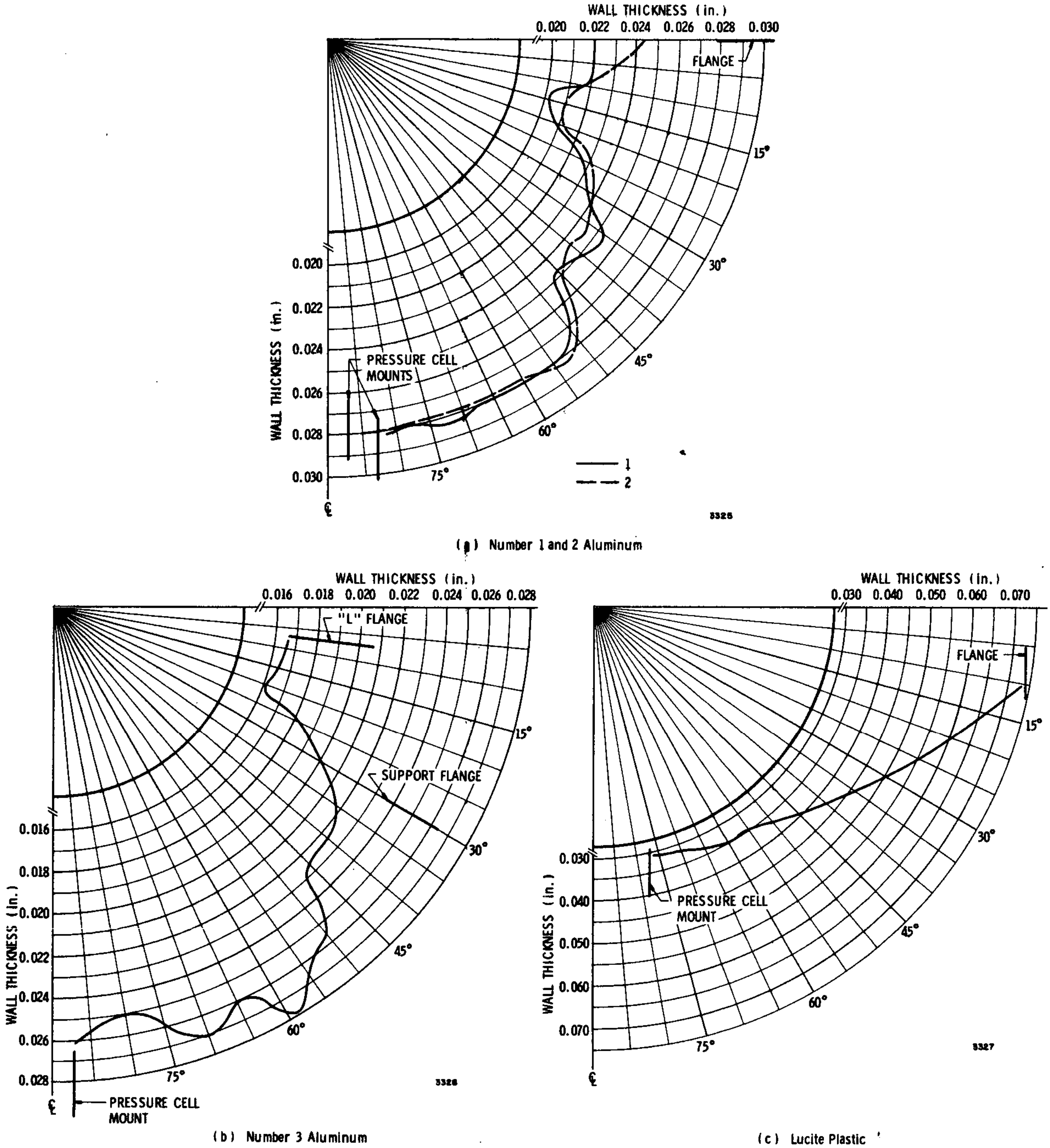

Figure 3. Wall Thickness Distribution for Hemispherical Bulkheads

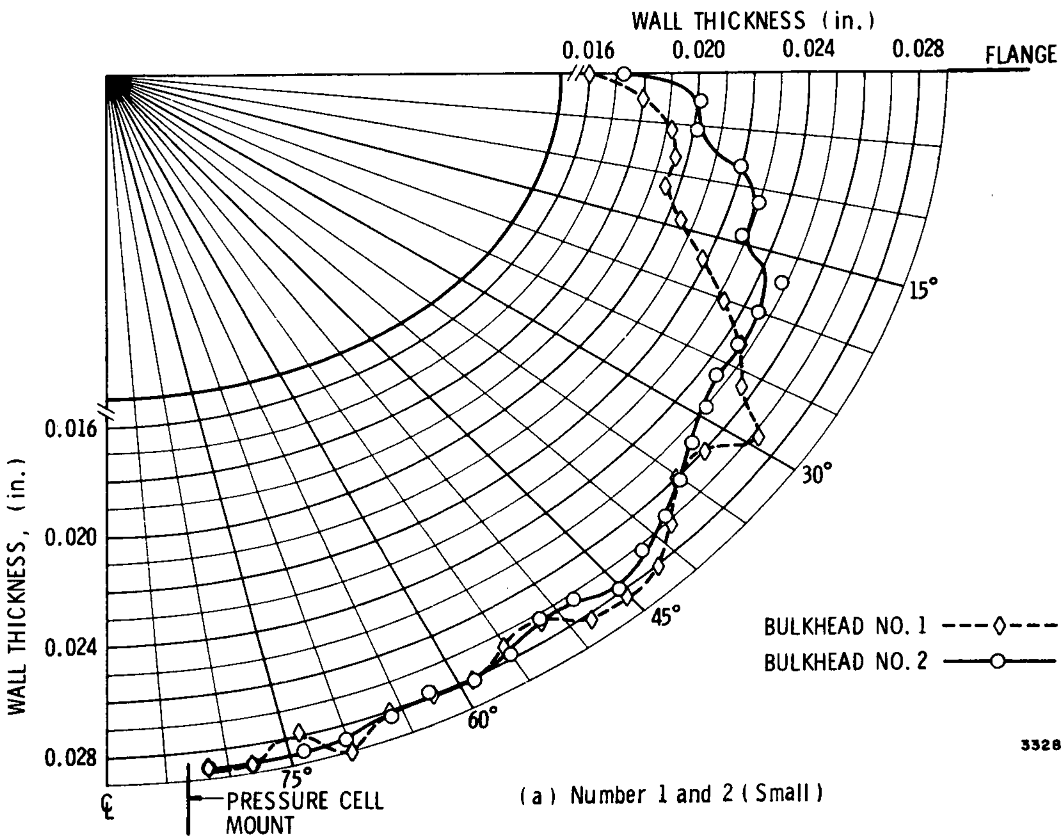

(a) Number 1 and 2 (Small)

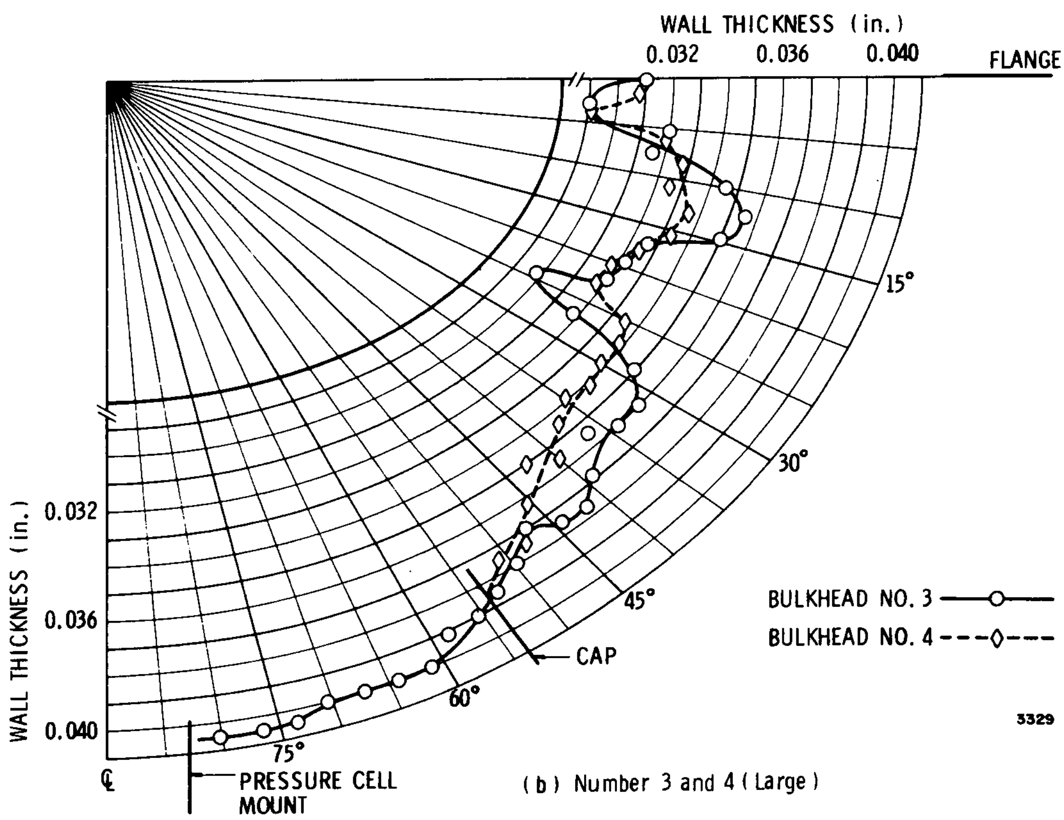

(b) Number 3 and 4 (Large)

Figure 4. Wall Thickness Distribution for Ellipsoidal Bulkheads

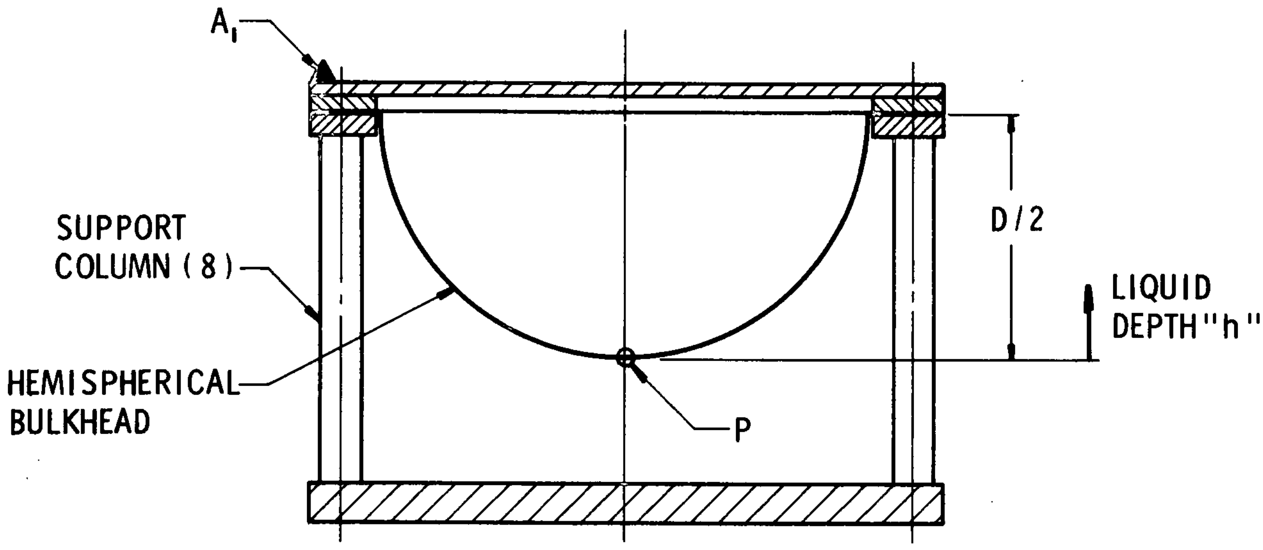

Structural Element	Equation of Surface	Inside Dia. (in.)	Wall Thickness (in.)	Material Density (#/in^3)	E x 10^6 psi
Bulkhead	$x^2 + y^2 = 5^2$	D = 10.0	Fig. 3	0.098	10

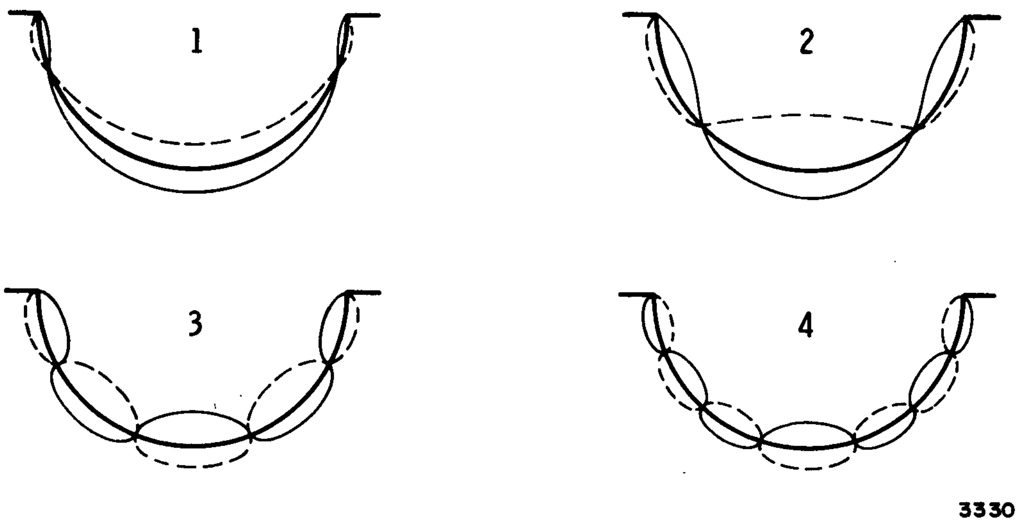

Figure 5. Aluminum Hemispherical Bulkheads and Mode Shapes

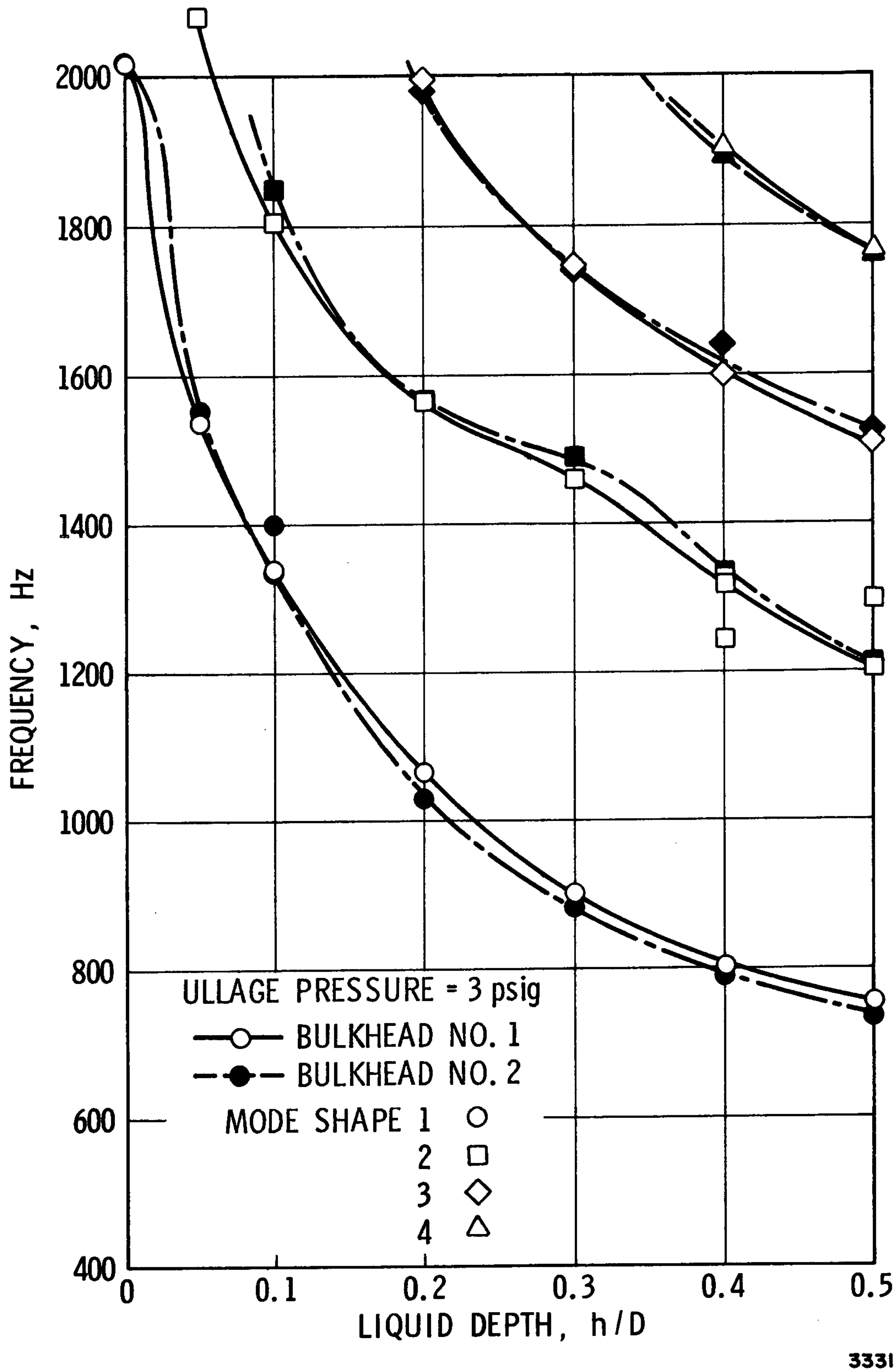

Figure 6. Natural Frequencies for Aluminum Hemispherical Bulkheads

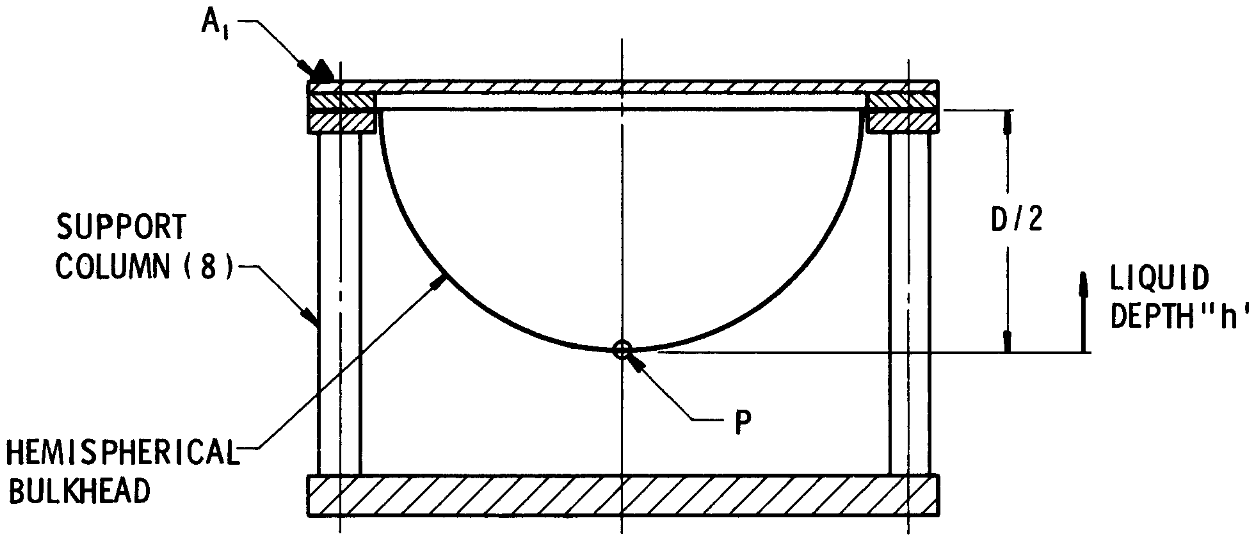

Structural Element	Equation of Surface	Inside Dia. (in.)	Wall Thickness (in.)	Material Density (#/in³)	E x 10^6 psi
Bulkhead	$x^2 + y^2 = 4.93^2$	D = 9.86	Fig. 3	0.043	0.4

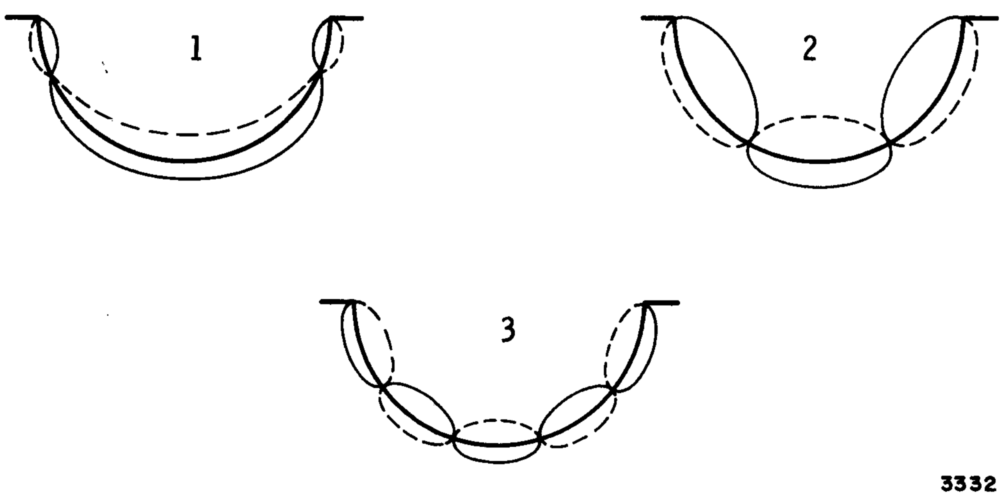

Figure 7. Plastic Hemispherical Bulkhead and Mode Shapes

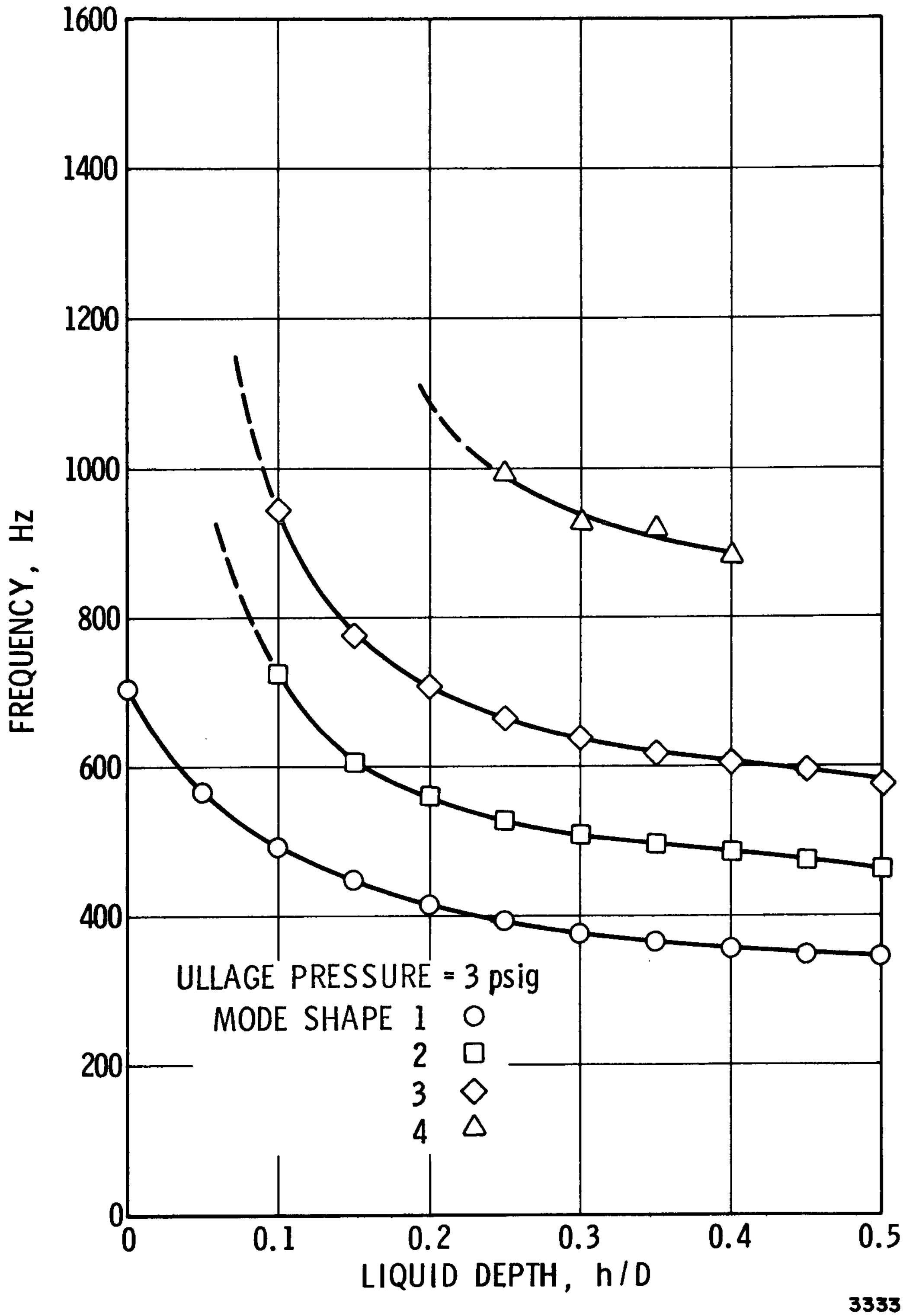

Figure 8. Natural Frequencies for Plastic Hemispherical Bulkhead

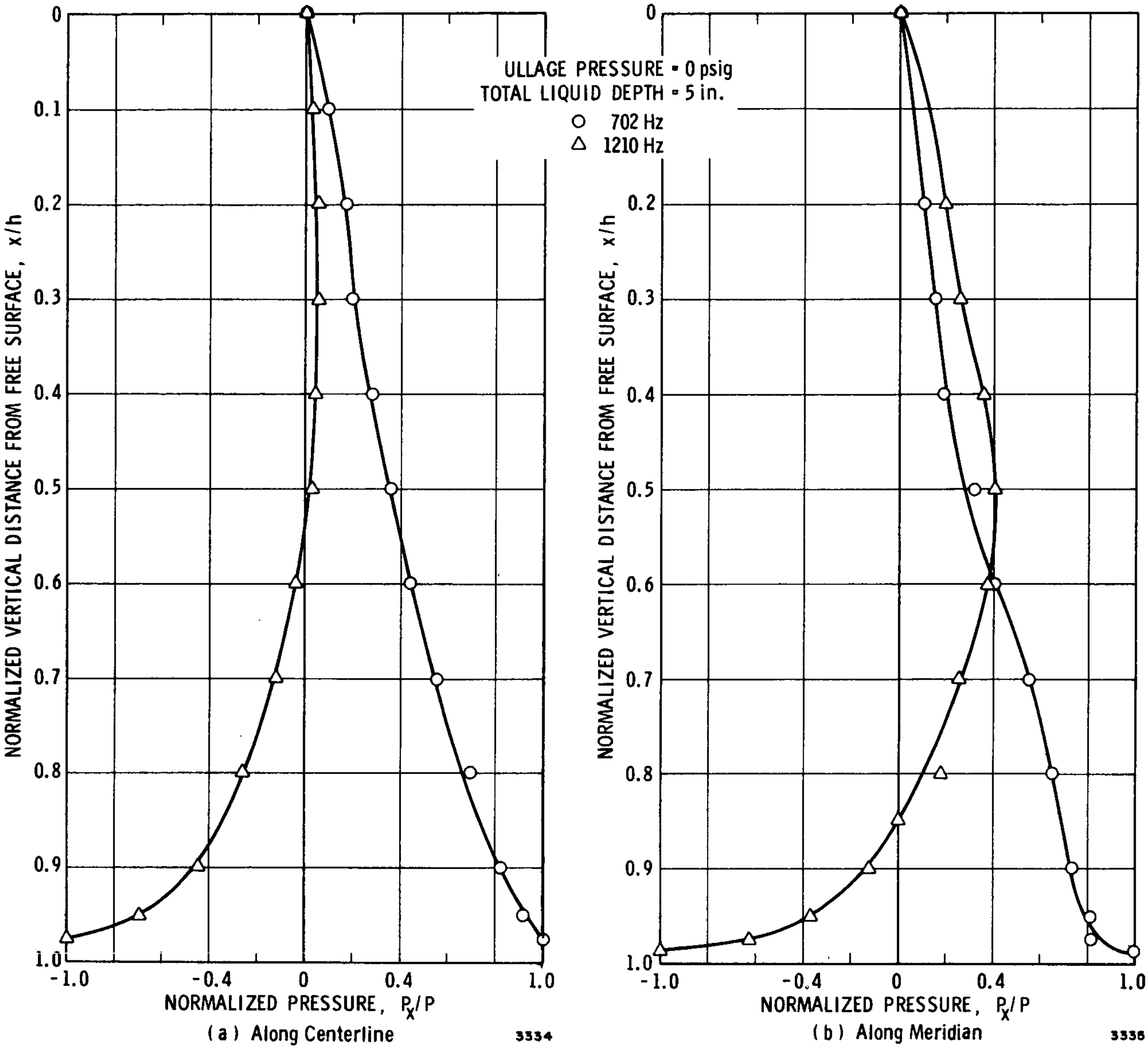

Figure 9. Pressure Profiles for Aluminum Hemispherical Bulkhead

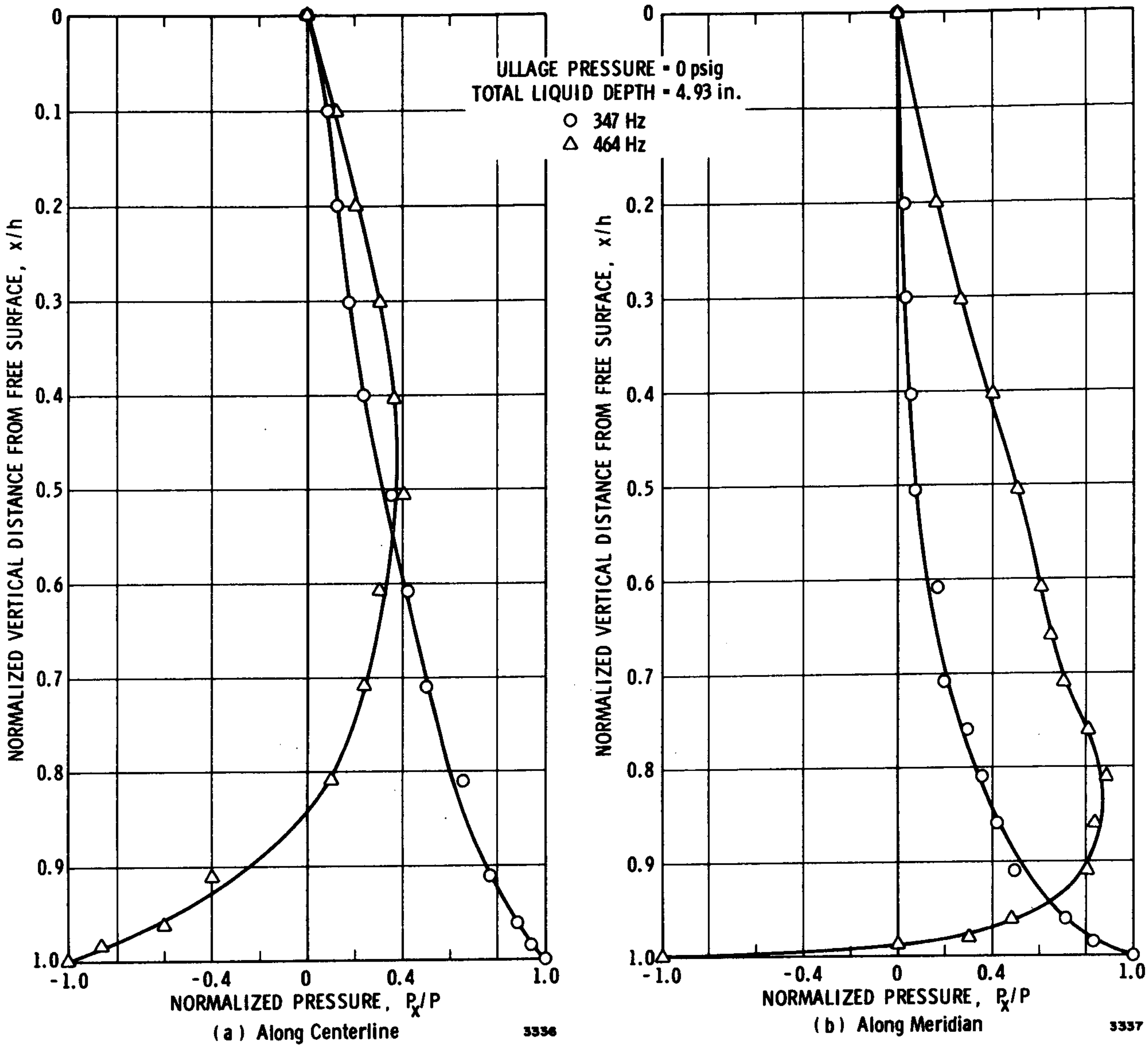

Figure 10. Pressure Profiles Plastic Hemispherical Bulkhead

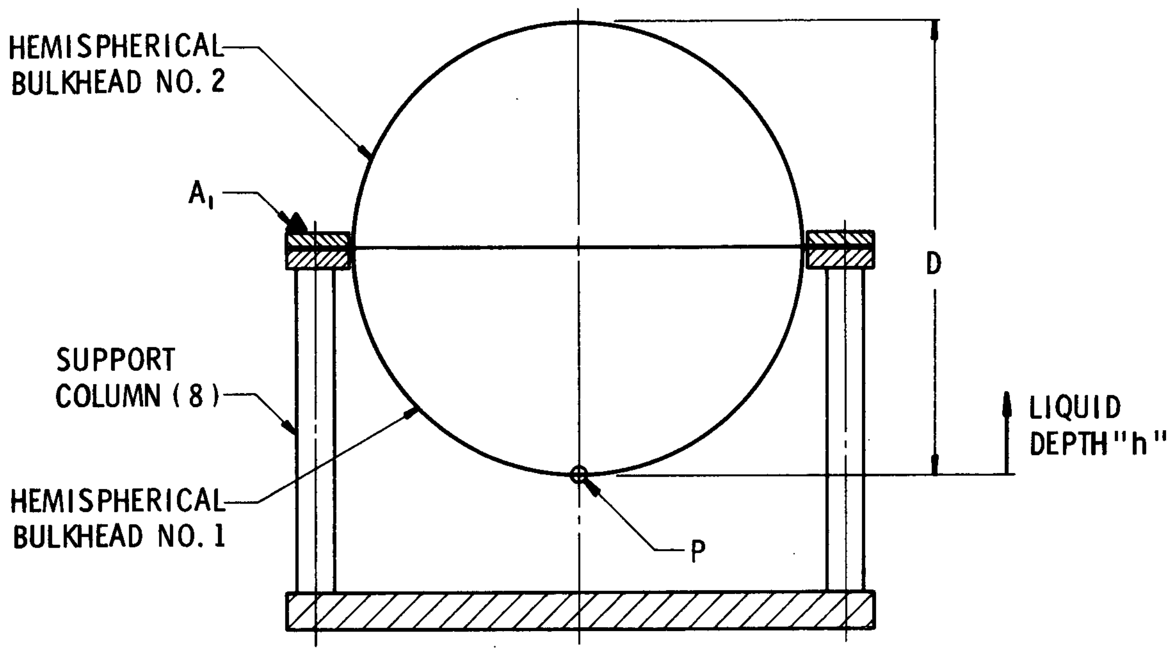

Structural Element	Equation of Surface	Inside Dia. (in.)	Wall Thickness (in.)	Material Density (#/in.^{3})	E x 10^6 psi
Bulkheads	$x^2 + y^2 = 5^2$	D = 10.0	Fig. 3	0.098	10

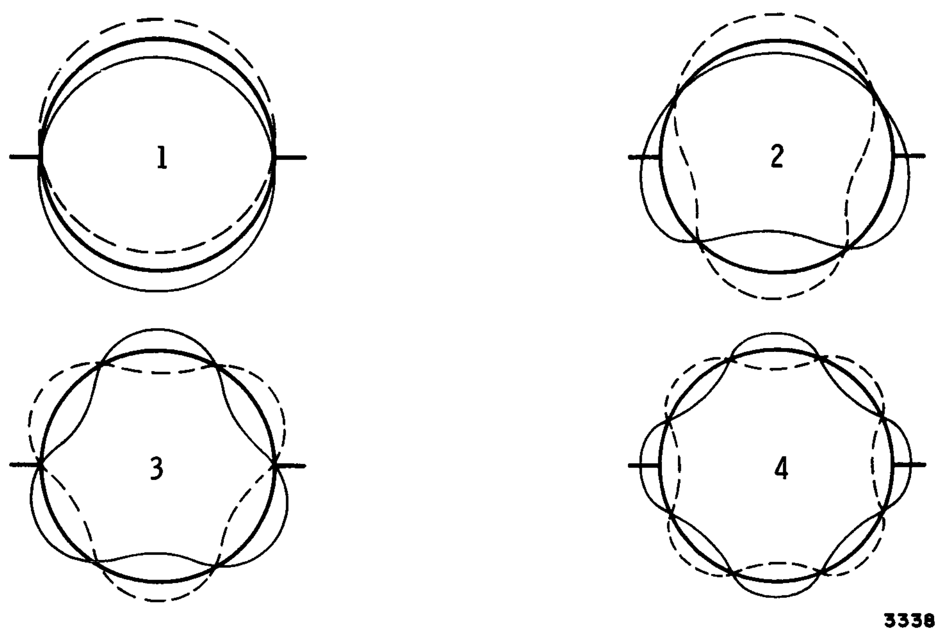

Figure 11. Spherical Tank Supported at Center Flange and Mode Shapes for Configuration 1

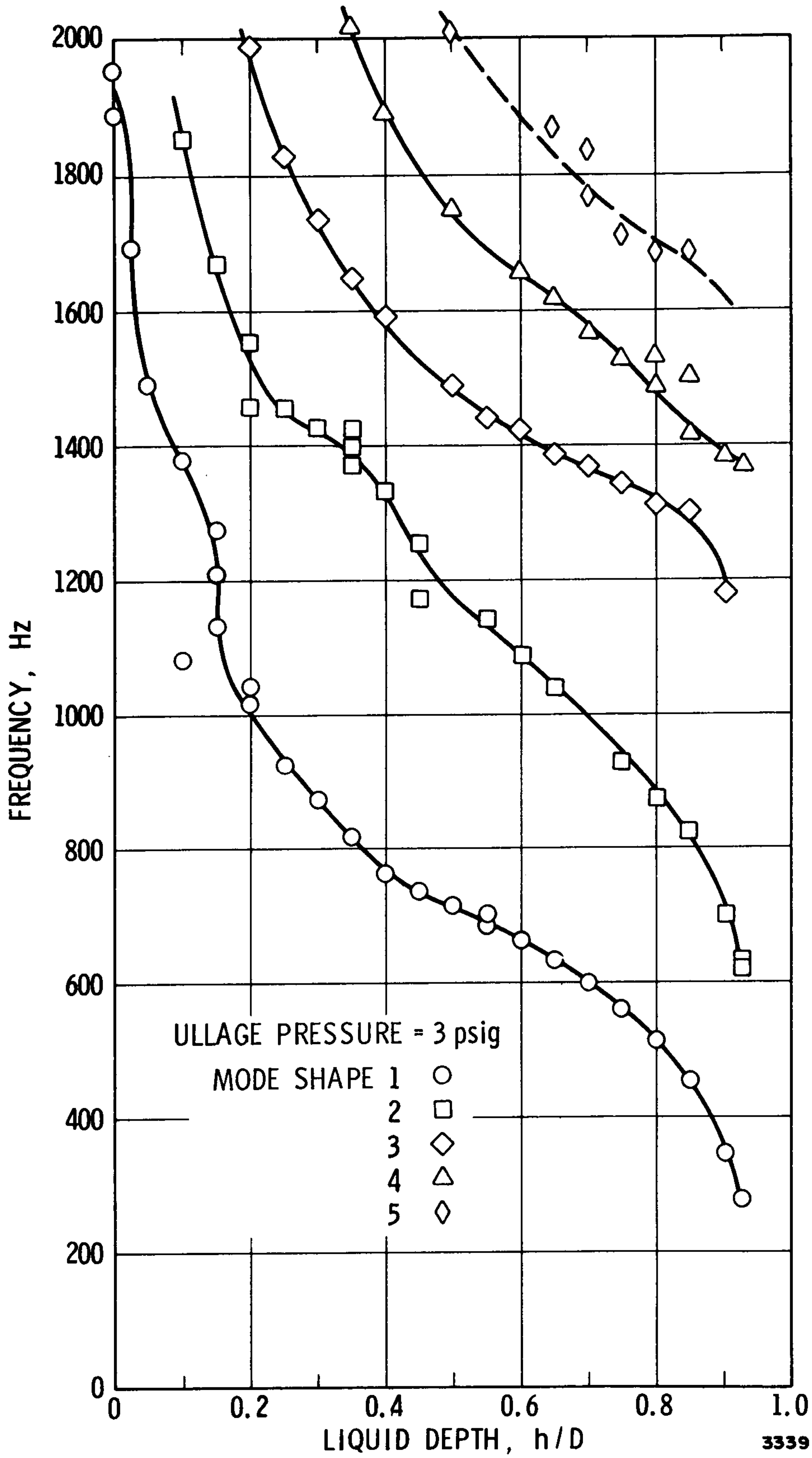

Figure 12. Natural Frequencies of Spherical Tank Supported at Center Flange for Configuration 1

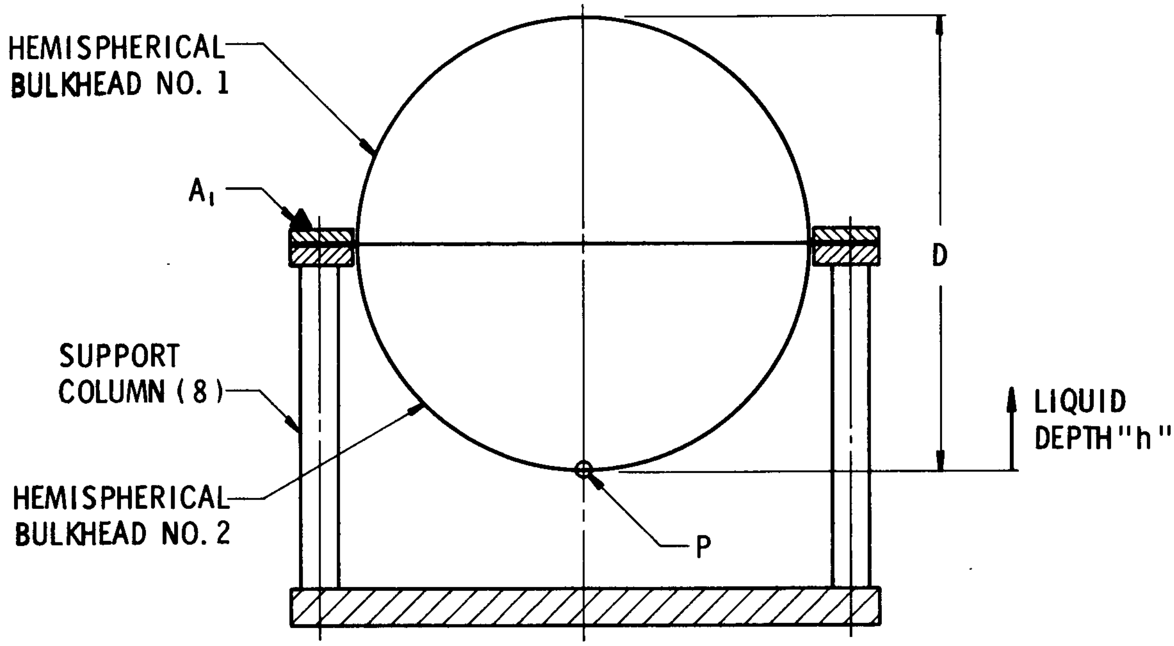

Structural Elements	Equation of Surface	Inside Dia. (in.)	Wall Thickness (in.)	Material Density (#/in^3)	E x 10^6 psi
Bulkheads	$x^2 + y^2 = 5^2$	D = 10.0	Fig. 3	0.098	10

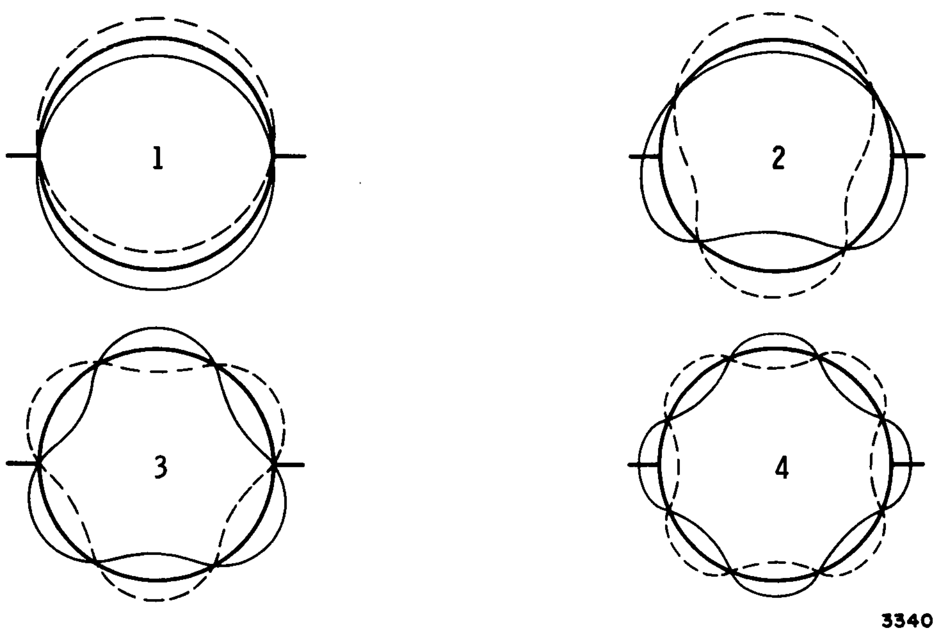

Figure 13. Spherical Tank Supported at Center Flange and Mode Shapes for Configuration 2

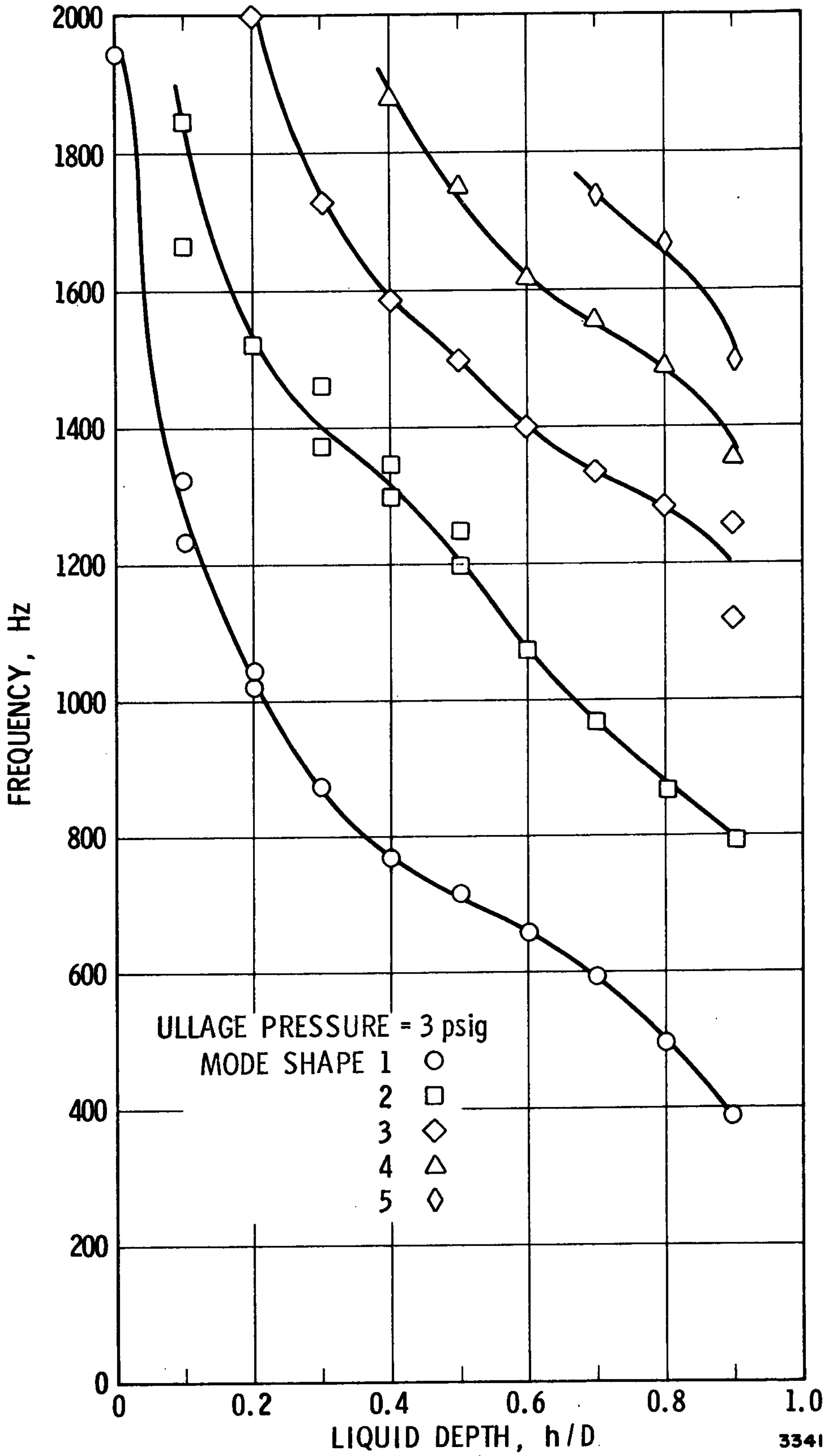

Figure 14. Natural Frequencies of Spherical Tank Supported at Center Flange for Configuration 2

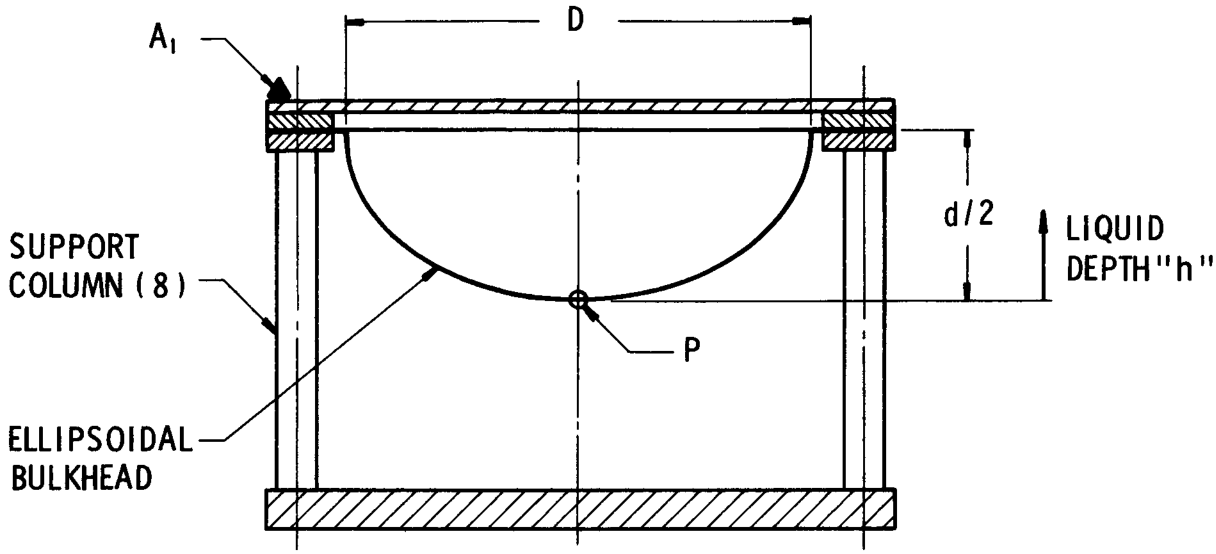

Structural Elements	Equation of Surface	Inside Dia. (in.)	Wall Thickness (in.)	Material Density (#/in.^{3})	E x 10^6 psi
Bulkheads	$\frac{x^2 + 2y^2}{5^2} = 1$	D = 10.0 d = 7.07	Fig. 4	0.098	10

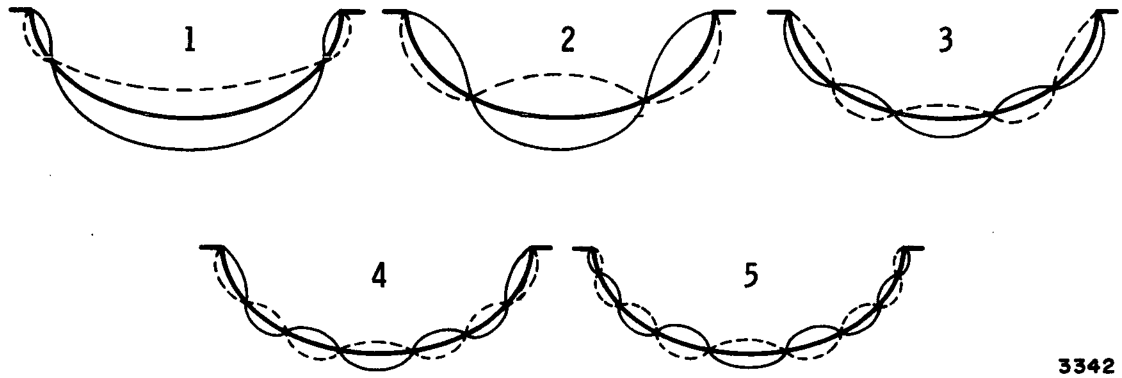

Figure 15. Small Ellipsoidal Bulkheads and Mode Shapes

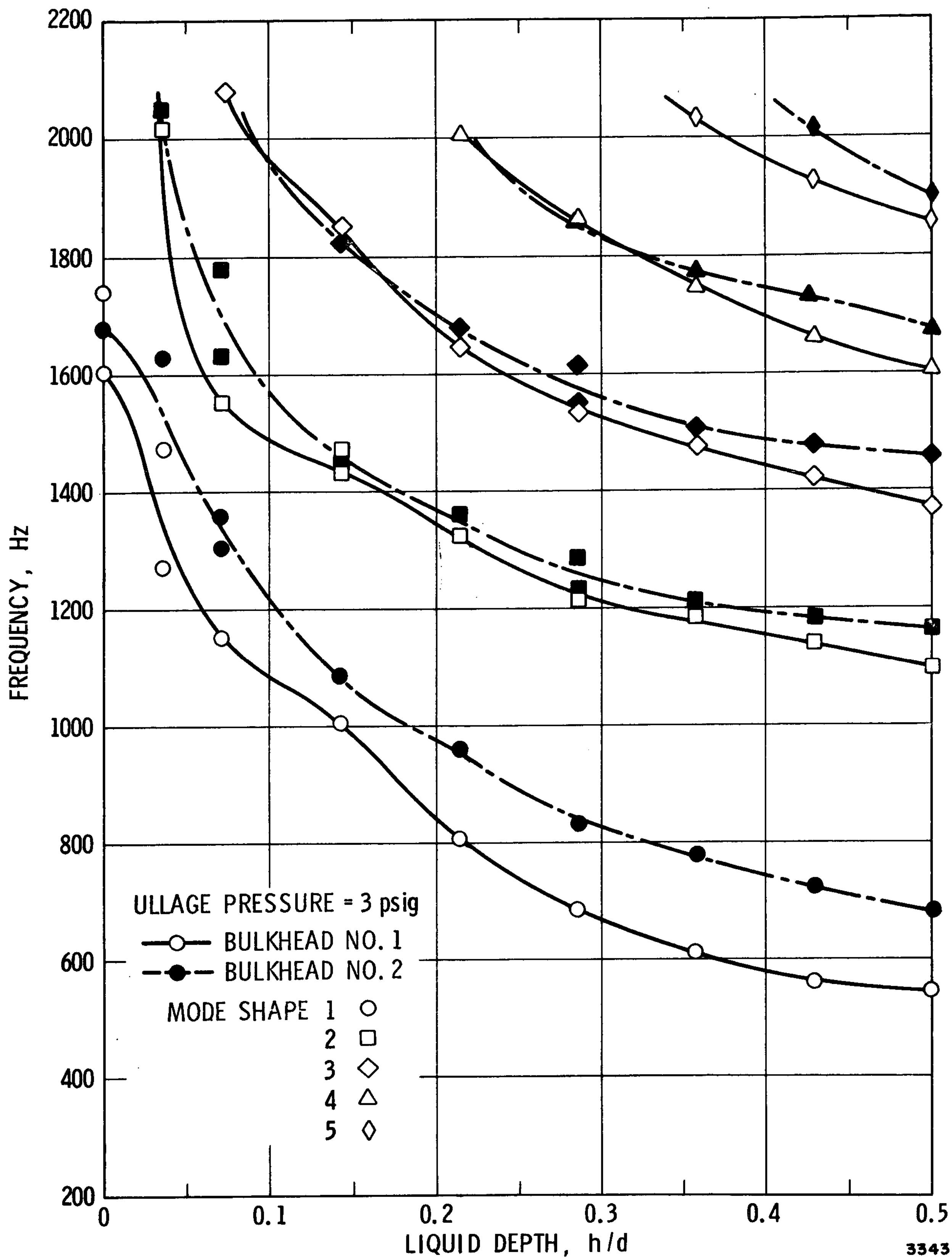

Figure 16. Natural Frequencies for Small Ellipsoidal Bulkheads

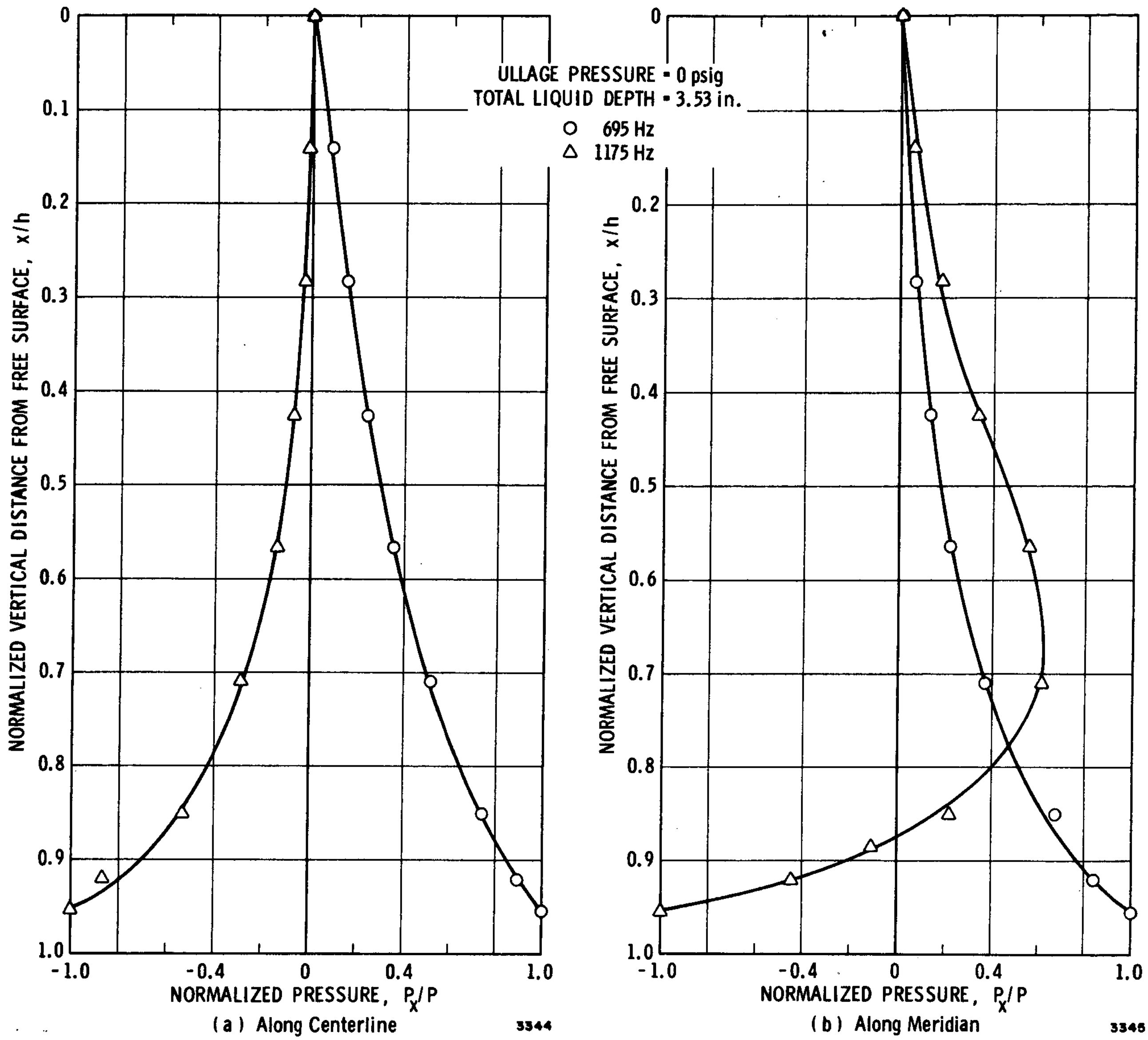

Figure 17. Pressure Profiles for Small Ellipsoidal Bulkhead

PRECEDING PAGE BLANK NOT FILMED

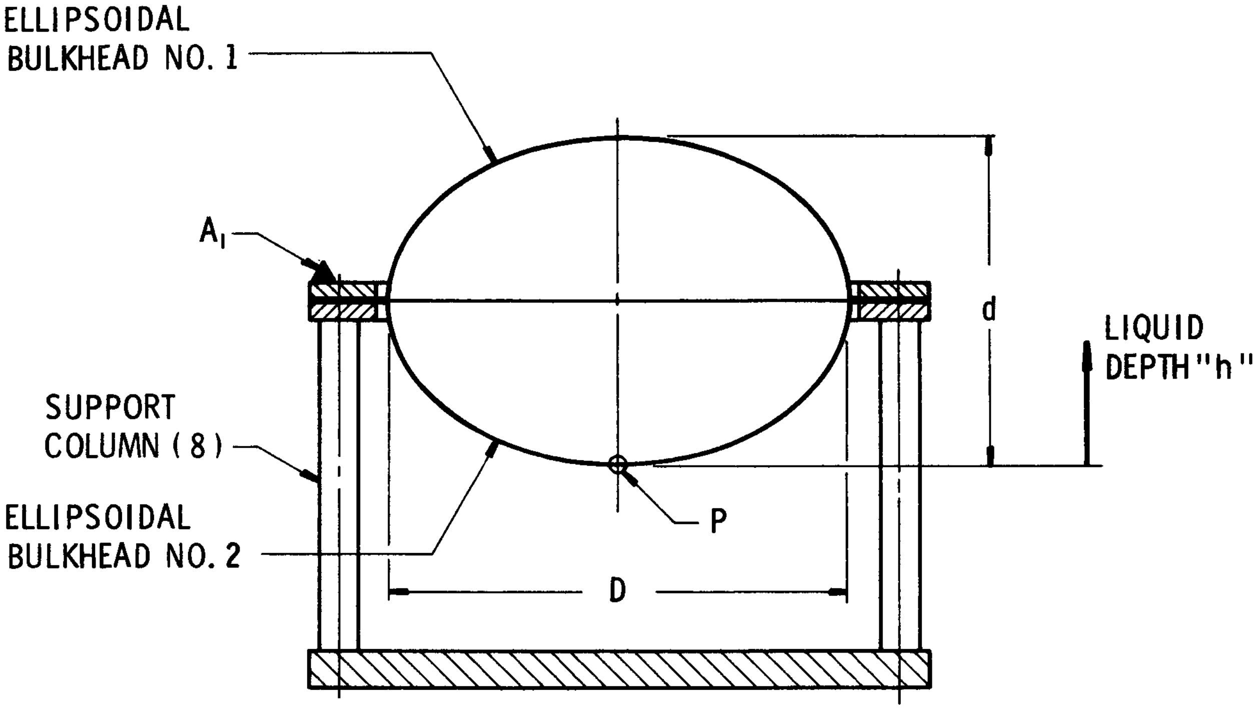

Structural Element	Equation of Surface	Inside Dia. (in.)	Wall Thickness (in.)	Material Density (#/in.^{3})	E x 10^6 psi
Bulkheads	$\frac{x^2+2y^2}{5^2}=1$	D = 10.0 d = 7.07	Fig. 4	0.098	10

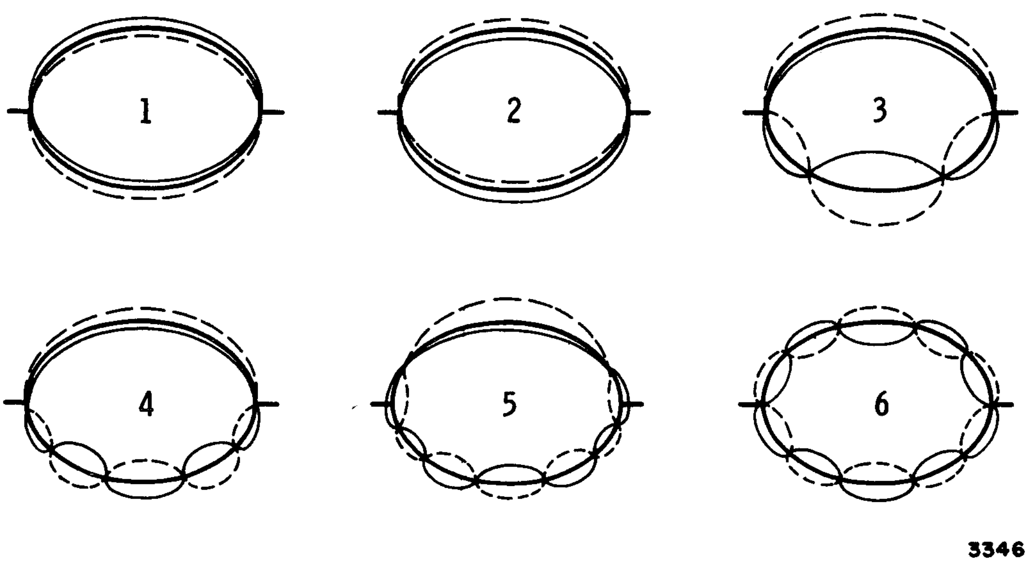

Figure 18. Small Ellipsoidal Tank and Mode Shapes

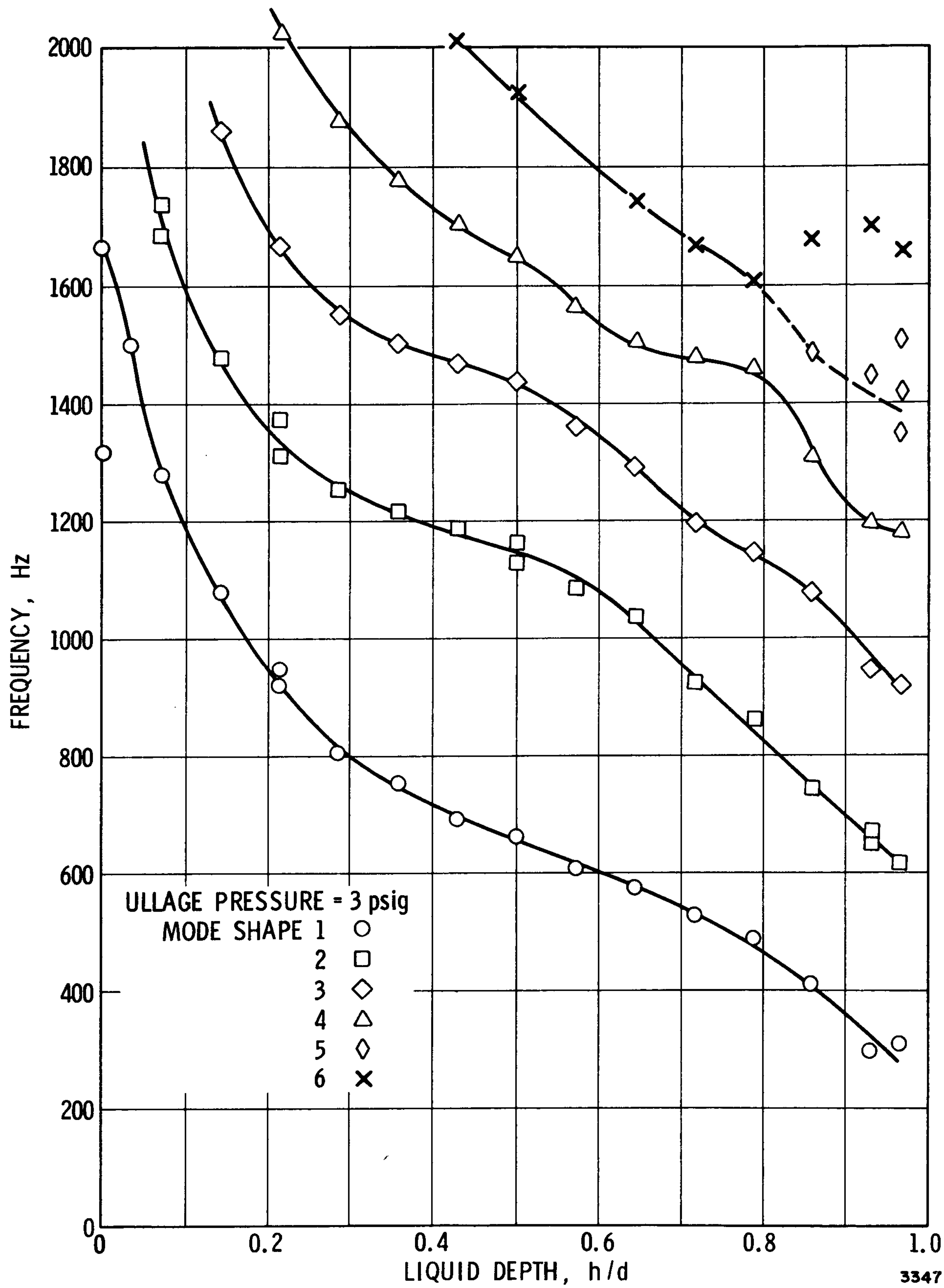

Figure 19. Natural Frequencies for Small Ellipsoidal Tank

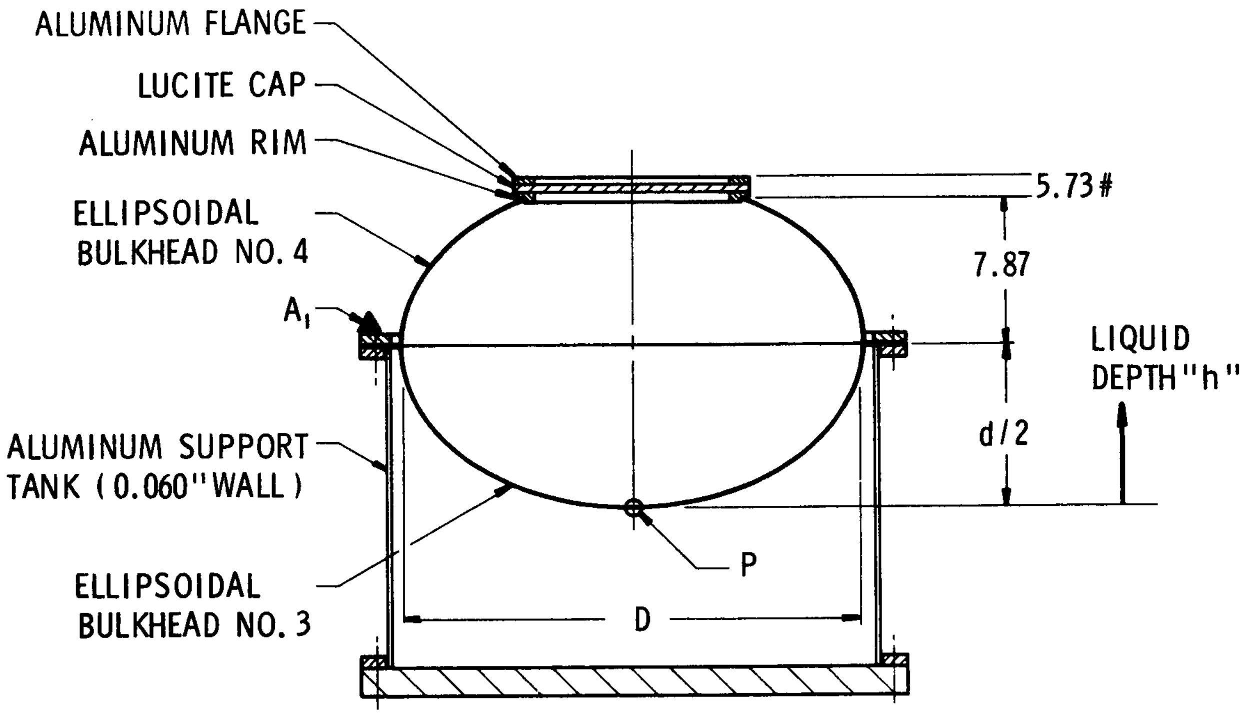

Structural Element	Equation of Surface	Inside Dia. (in.)	Wall Thickness (in.)	Material Density (#/in.^{3})	E x 10^6 psi
Bulkheads	$\frac{x^2 + 2y^2}{12.375^2} = 1$	D = 24.75 d = 17.5	Fig. 4	0.098	10

SYMBOLS USED FOR INDICATING GENERAL
MODE SHAPES ON LARGE ELLIPSOIDAL TANK

MODE	SYMBOL
1	●
2	○
3	□
4	■
5	◇
6	◆
7	⬙
8	△
9	▲

MODE	SYMBOL
10	◇
11	◆
12	◿
13	◢
14	◿
15	◇
16	◆
17	⬙
18	⌂

MODE	SYMBOL
19	⬟
20	⬟
21	⬡
22	⬢
23	⬢
24	⬯
25	⬮
26	◿
27	◢

3348

Figure 20. Large Ellipsoidal Tank

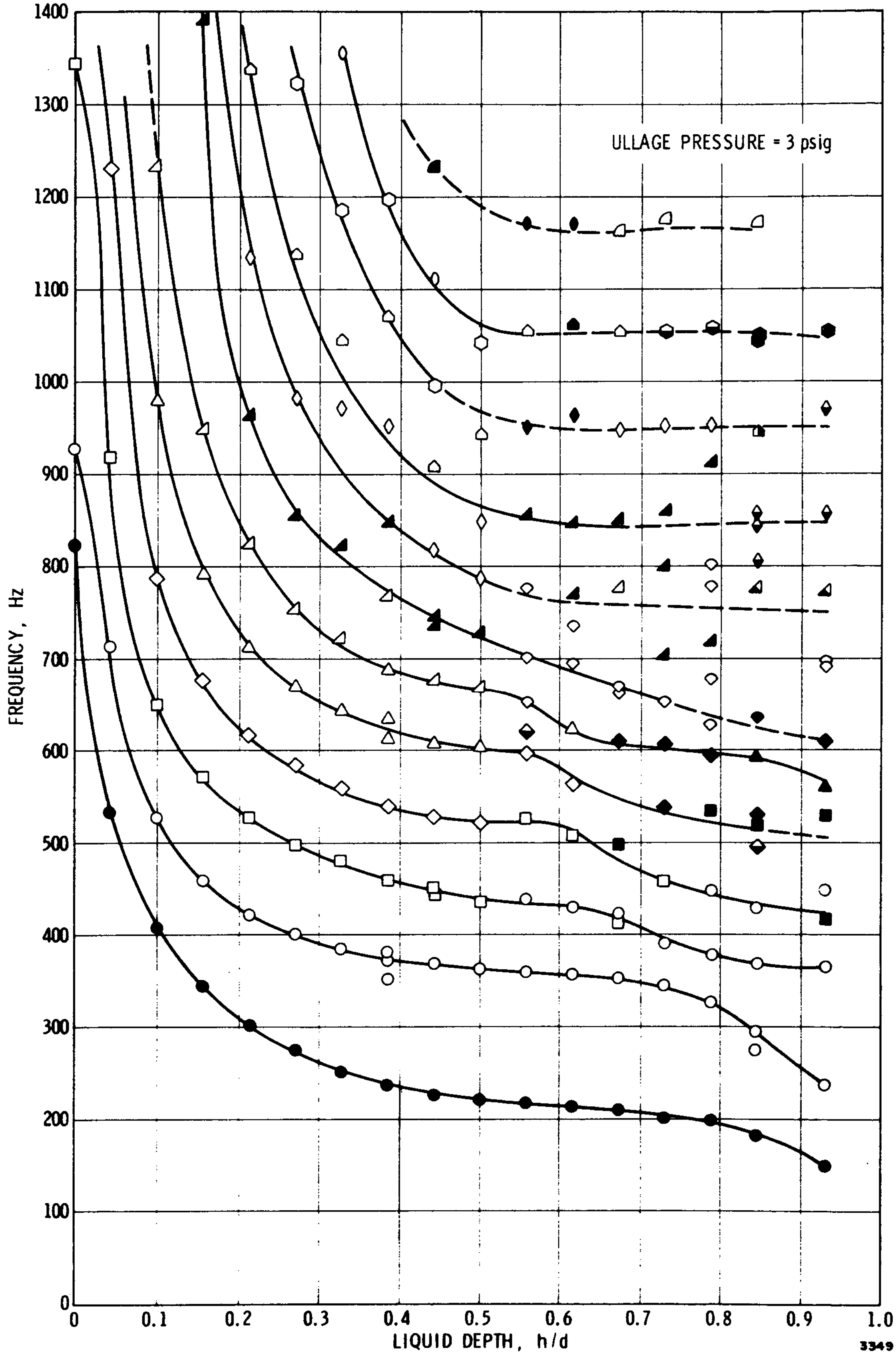

Figure 21. Natural Frequencies for Large Ellipsoidal Tank

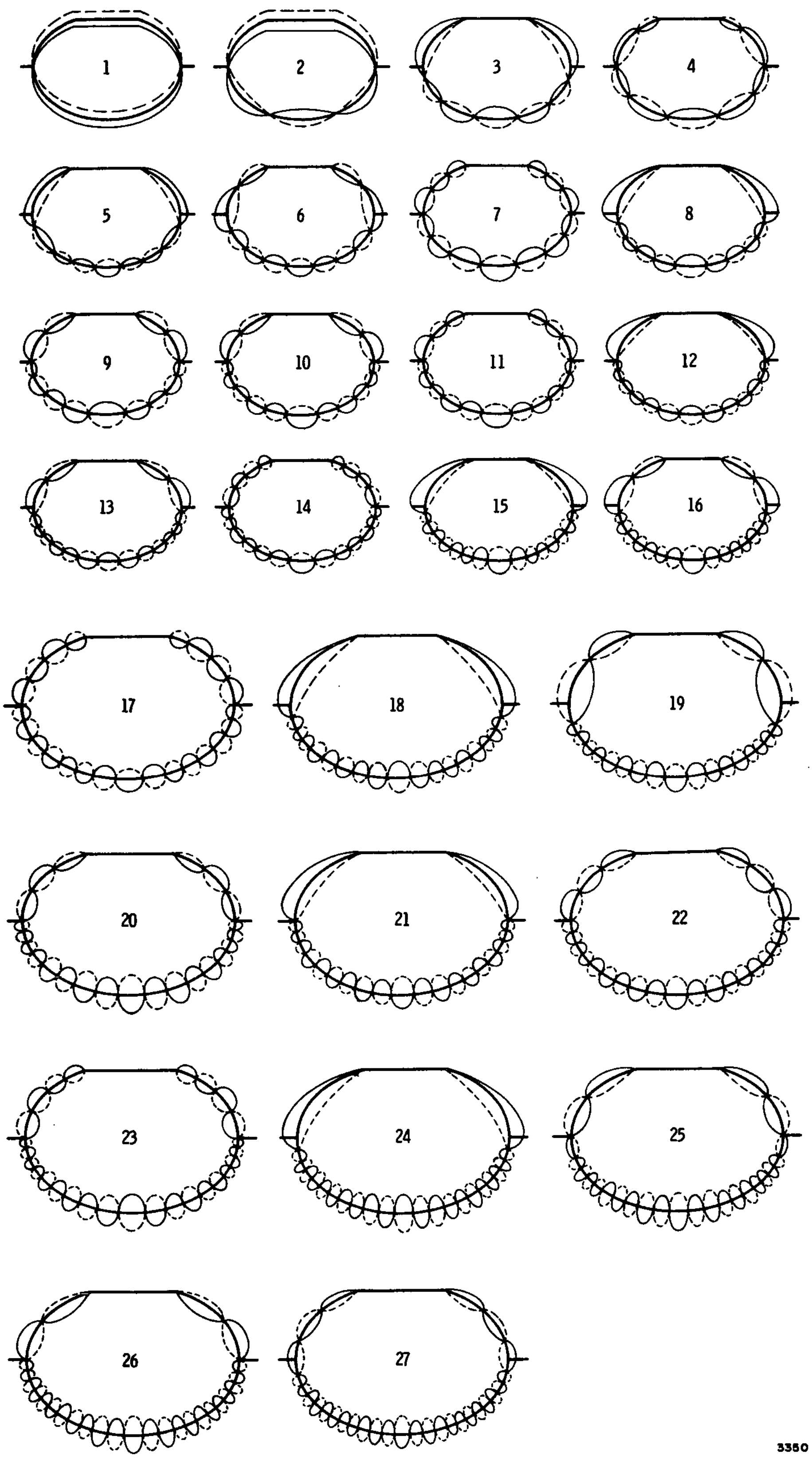

Figure 22. Mode Shapes for Large Ellipsoidal Tank

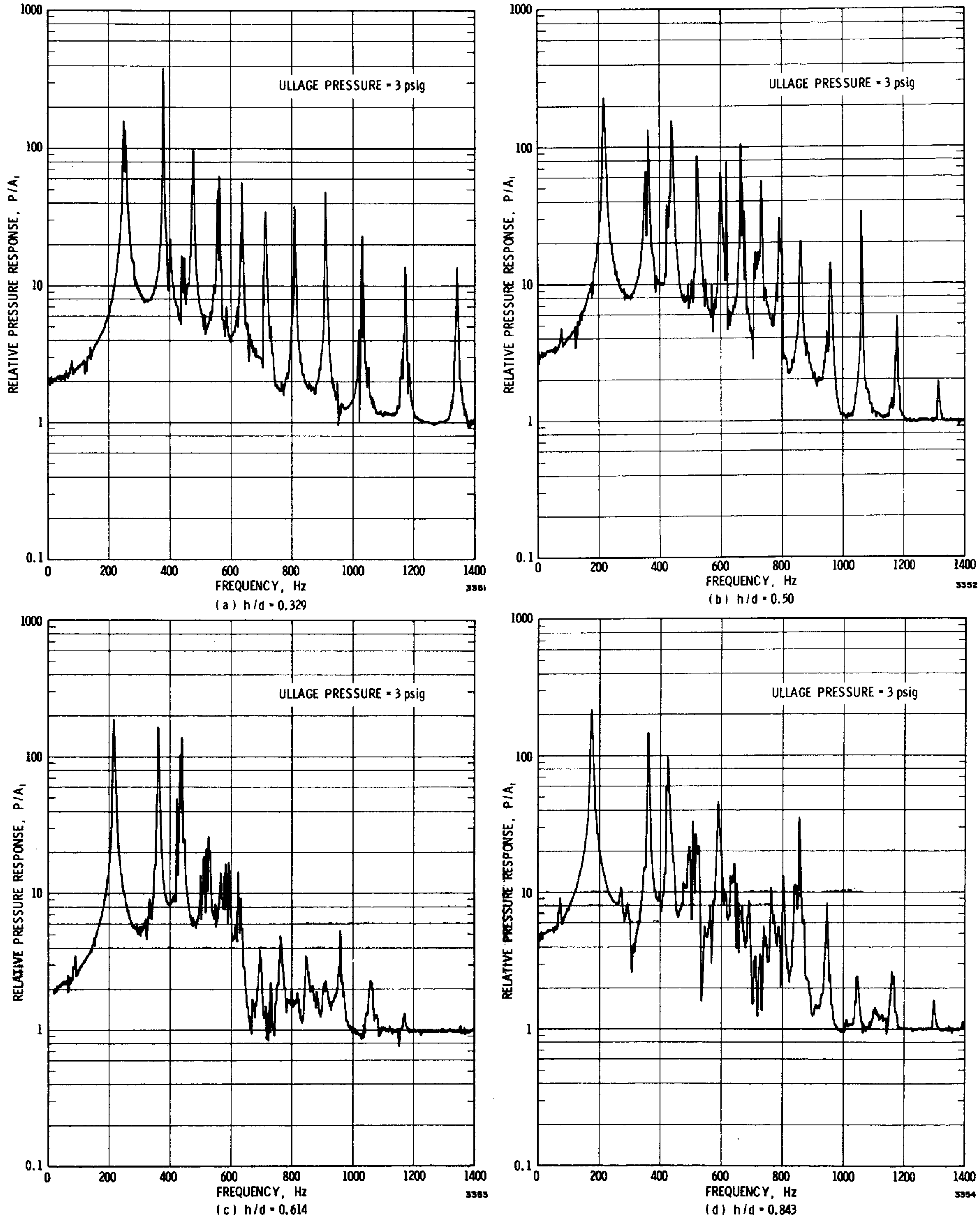

Figure 23. Relative Pressure Response for Large Ellipsoidal Tank

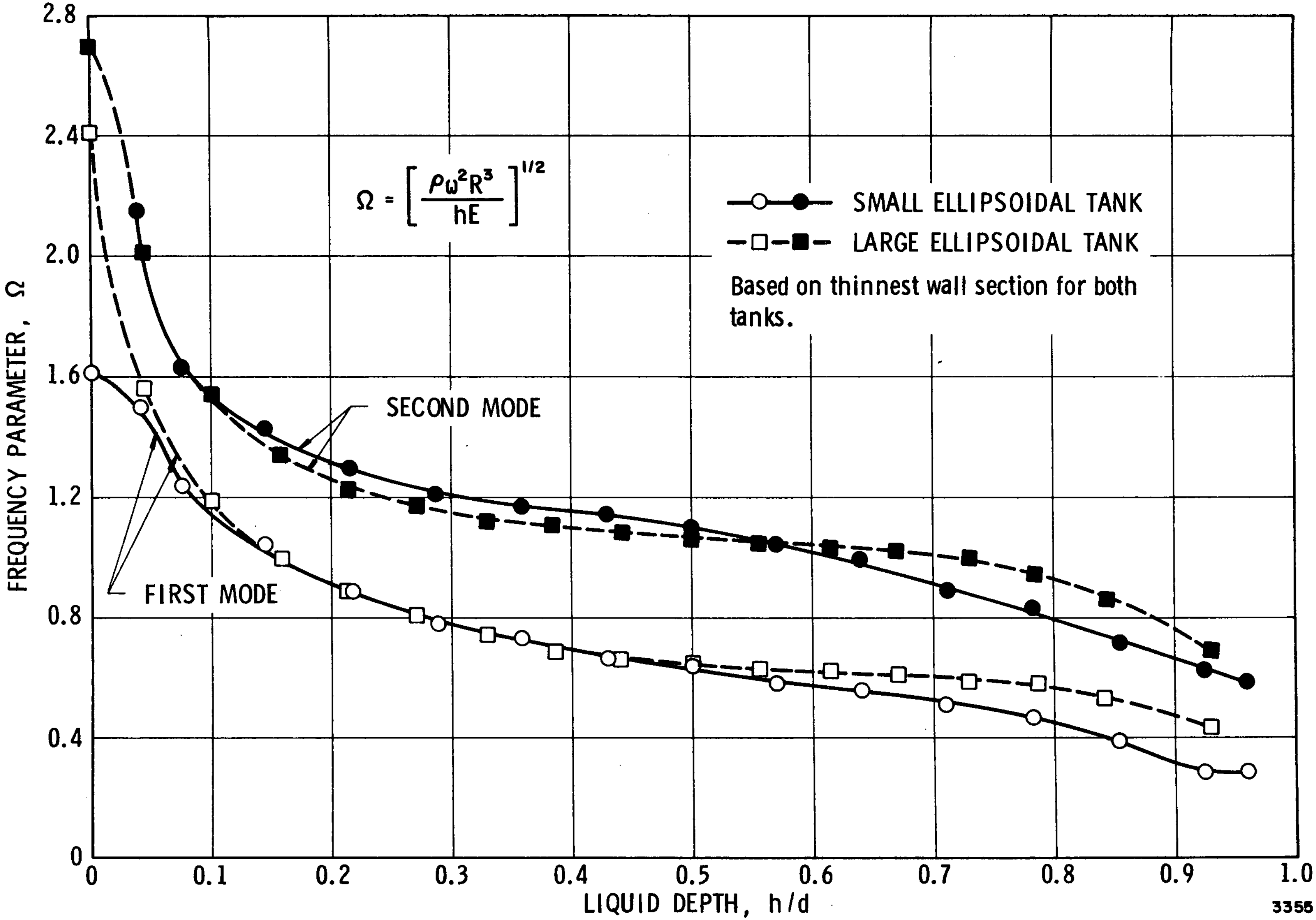

Figure 24. Comparison of Natural Frequencies for Large and Small Ellipsoidal Tanks

PRECEDING PAGE BLANK NOT FILMED

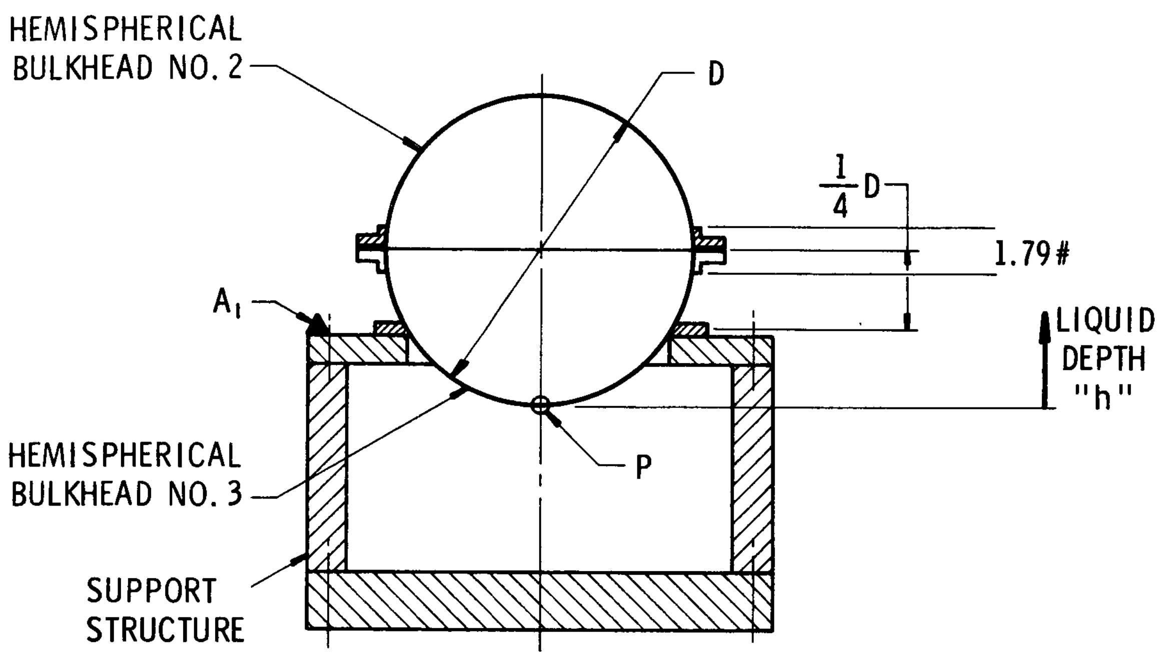

Structural Element	Equation of Surface	Inside Dia. (in.)	Wall Thickness (in.)	Material Density (#/in^3)	E x 10^6 psi
Bulkheads	$x^2 + y^2 = 5^2$	D = 10.0	Fig. 3	0.098	10

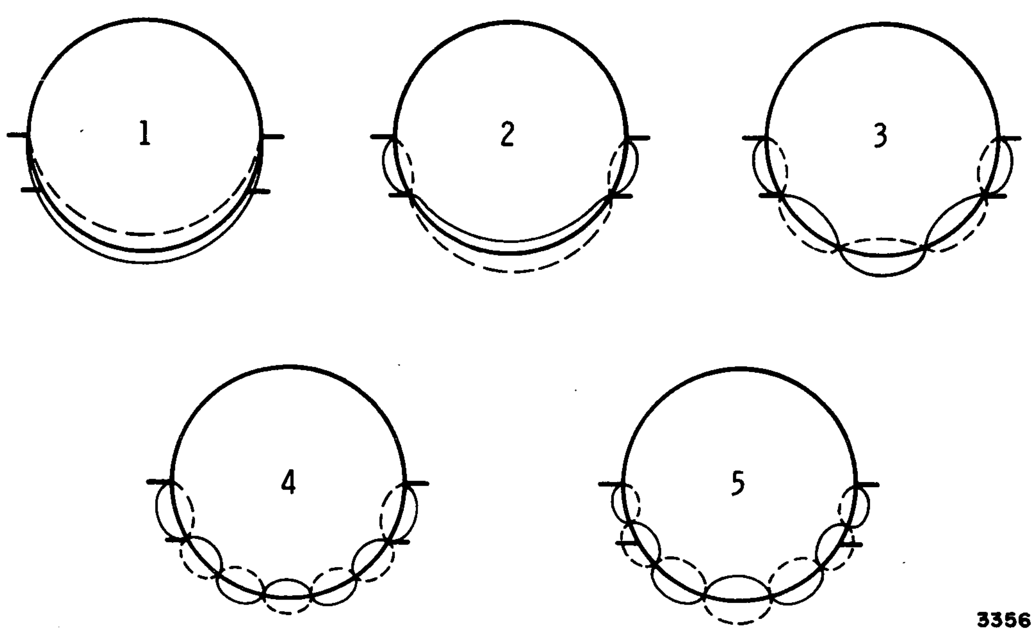

Figure 25. Spherical Tank and Mode Shapes for Support at Lower Half-Radius

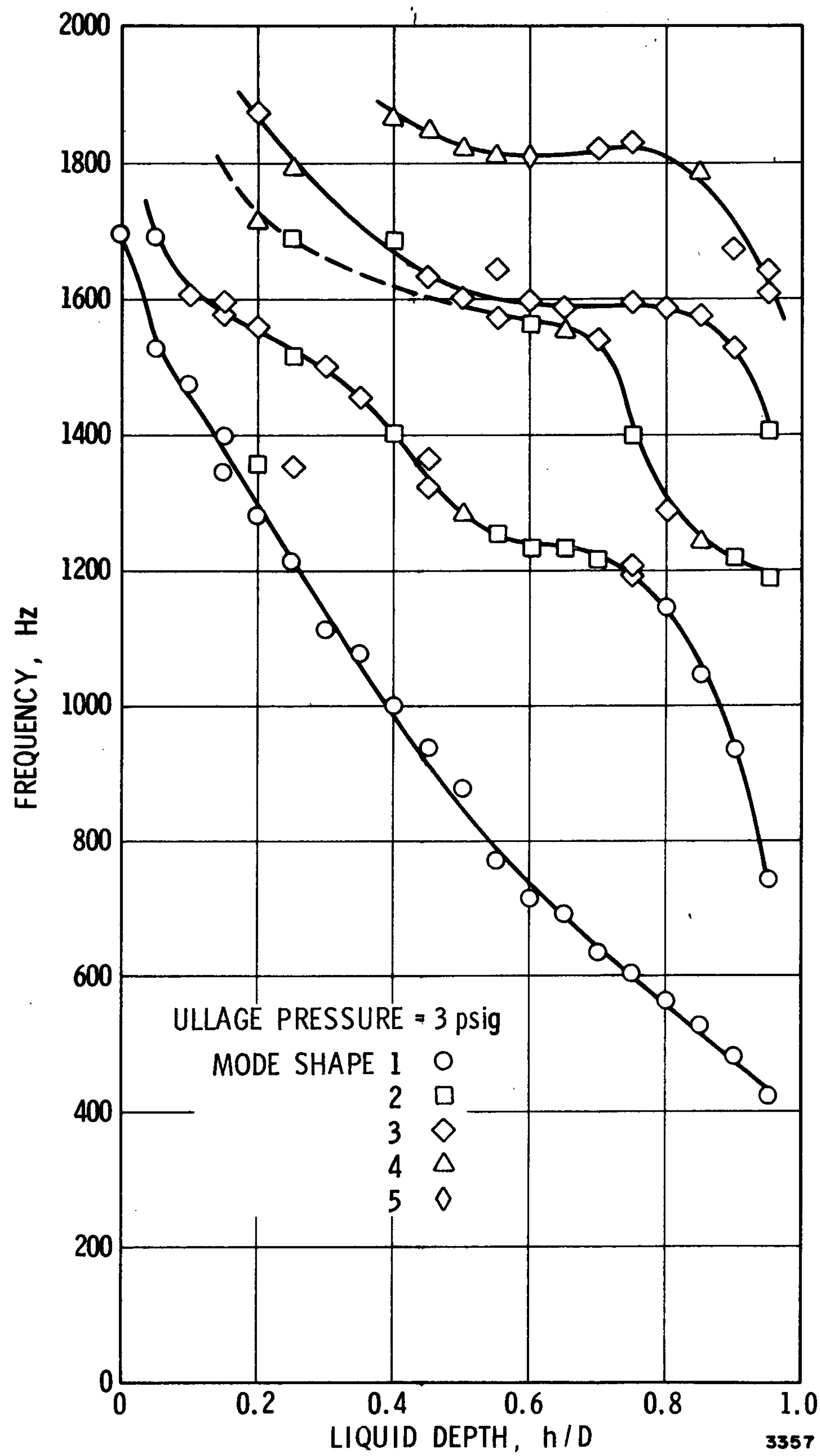

Figure 26. Natural Frequencies for Spherical Tank with Support at Lower Half-Radius

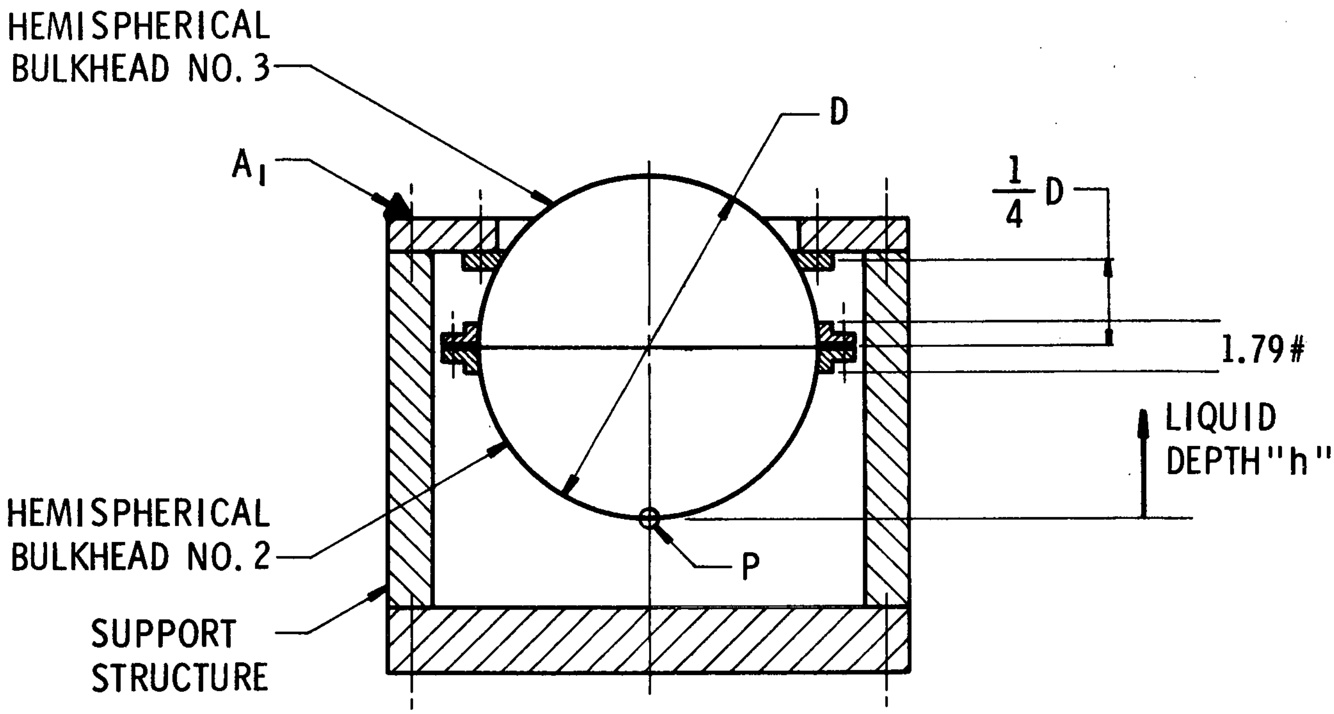

Structural Element	Equation of Surface	Inside Dia. (in.)	Wall Thickness (in.)	Material Density (#/in.^{3})	E x 10^6 psi
Bulkheads	$x^2 + y^2 = 5^2$	D = 10.0	Fig. 3	0.098	10

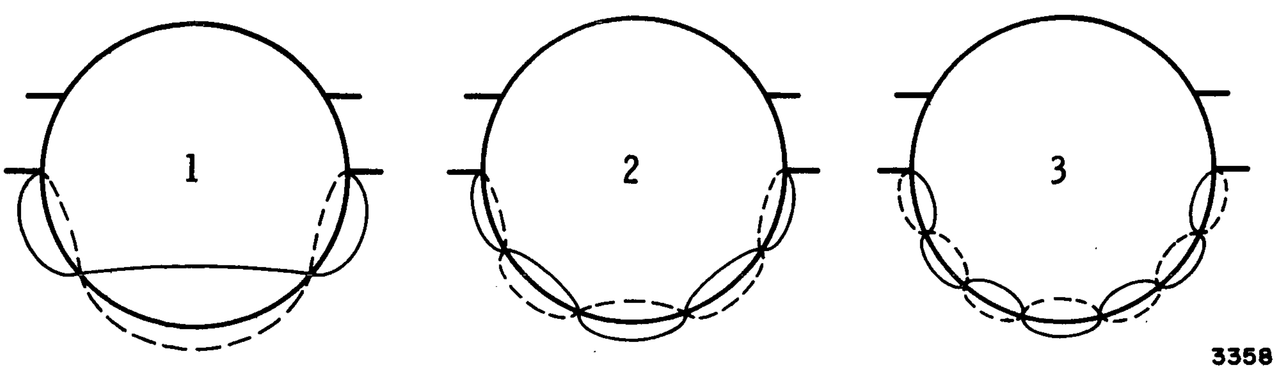

Figure 27. Spherical Tank and Mode Shapes for Support at Upper Half-Radius

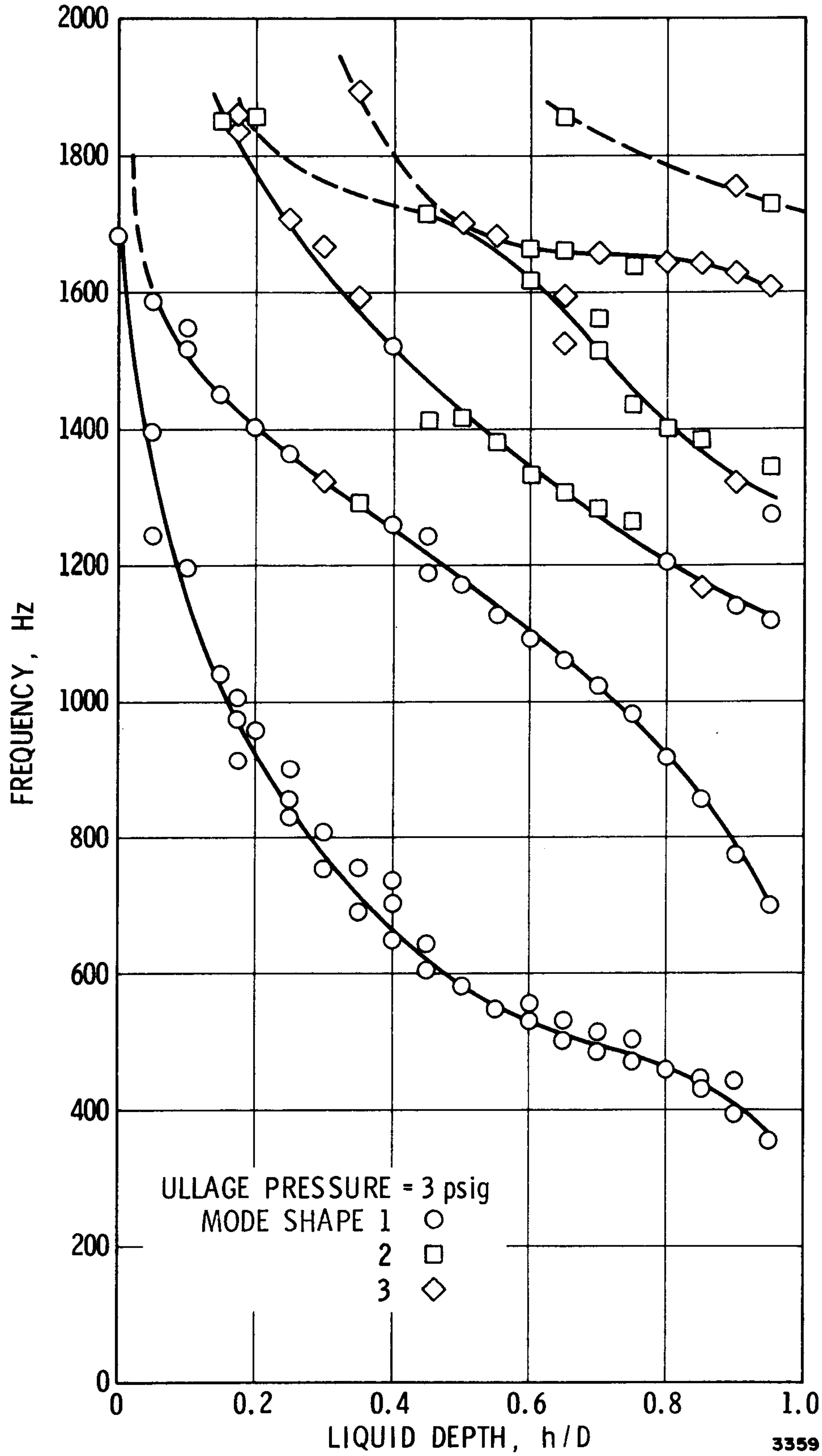

Figure 28. Natural Frequencies for Spherical Tank with Support at Upper Half-Radius

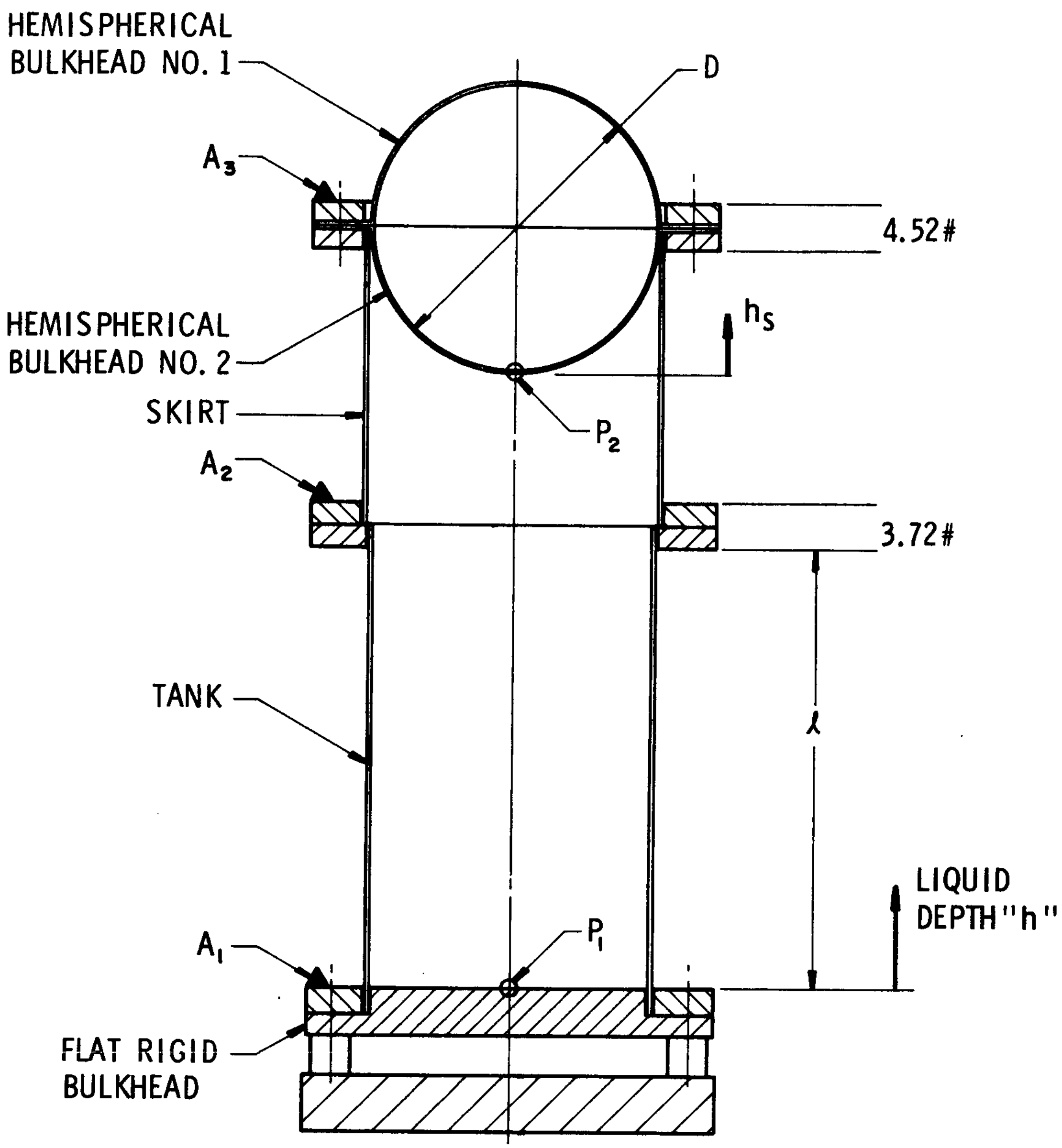

Structural Element	Effective Length (λ) (in.)	Inside Dia. (in.)	Wall Thickness (in.)	Material Density (#/in.^{3})	E x 10^6 psi
Tank Skirt	14.5 7.5	10.0 10.3	0.005 0.025	0.29 0.098	29 10
Bulkheads		D = 10.0	Fig. 3	0.098	10

3360

Figure 29. Cylinder and Sphere Tandem Configuration

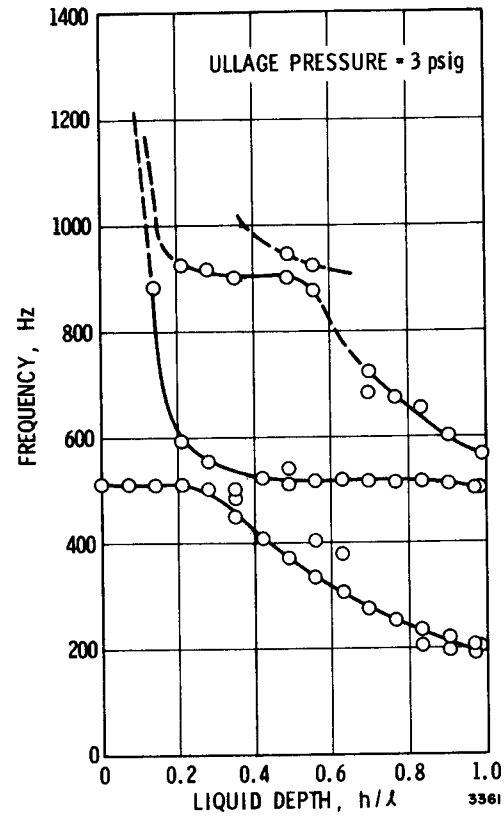

(a) Sphere Liquid Depth $h_S/D = 0$

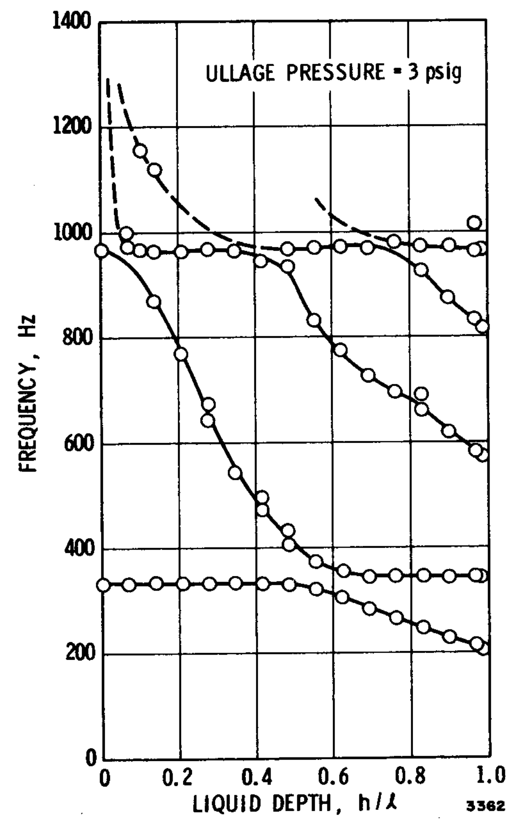

(b) Sphere Liquid Depth $h_S/D = 0.5$

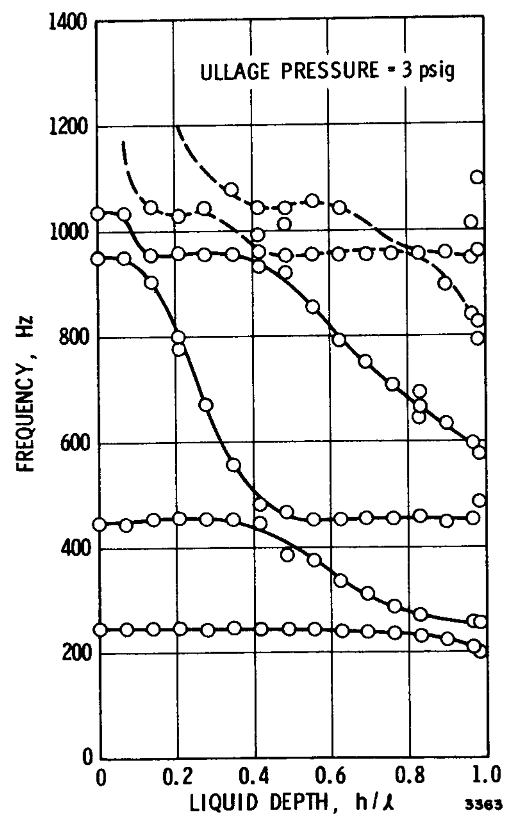

(c) Sphere Liquid Depth $h_S/D = 0.95$

Figure 30. Natural Frequencies for Cylinder and Sphere Tandem Configuration

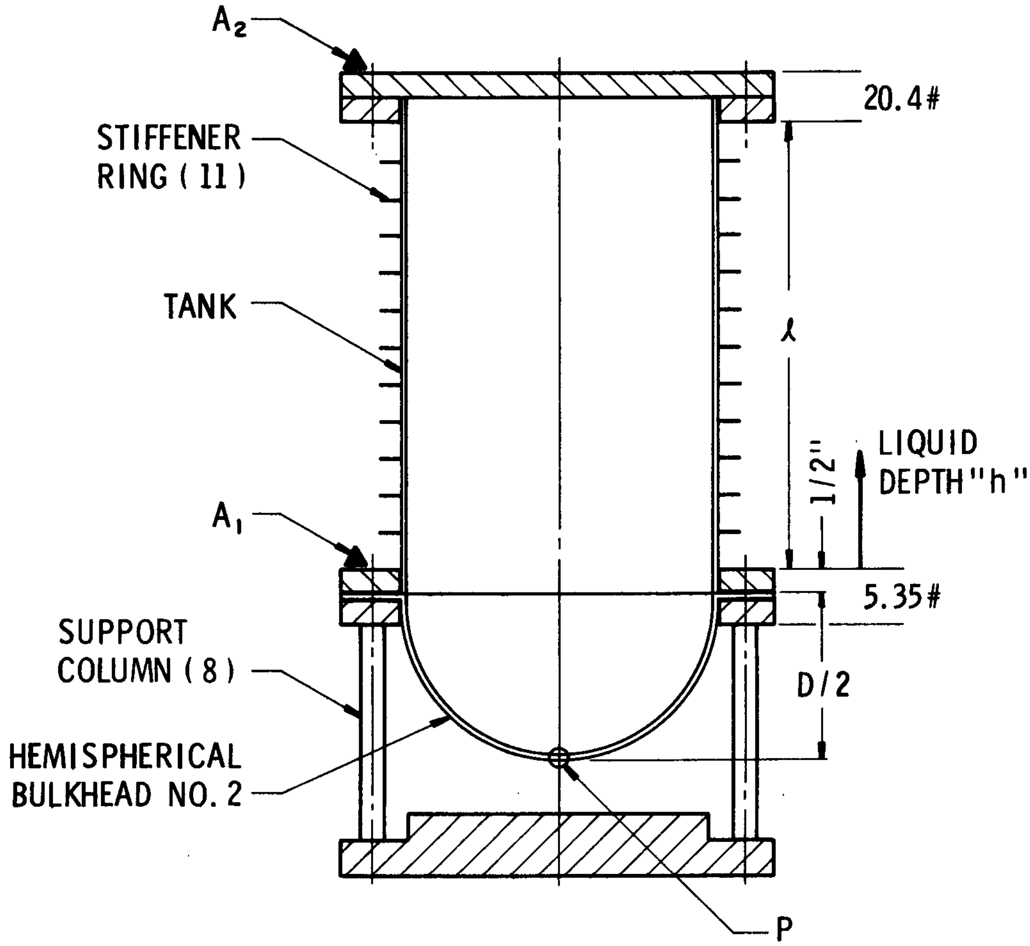

Structural Element	Effective Length (λ) (in.)	Inside Dia. (in.)	Wall Thickness (in.)	Material Density (#/in^3)	E x 10^6 psi
Tank	14.5	10.0	0.005	0.29	29
Bulkhead		D = 10.0	Fig. 3	0.098	10

Structural Element	Number Used On Tank	Material Density (#/in^3)	E x 10^6 psi	Dimensions (in.)	Location	Spacing (in.)
Stiffener Ring	11	0.098	10	10.0 I.D. 10.5 O.D. 0.032 Thick	Symmetrical about midspan	1.24

3364

Figure 31. Cylindrical Tank with Hemispherical Bulkhead-Stiffener Rings Configuration

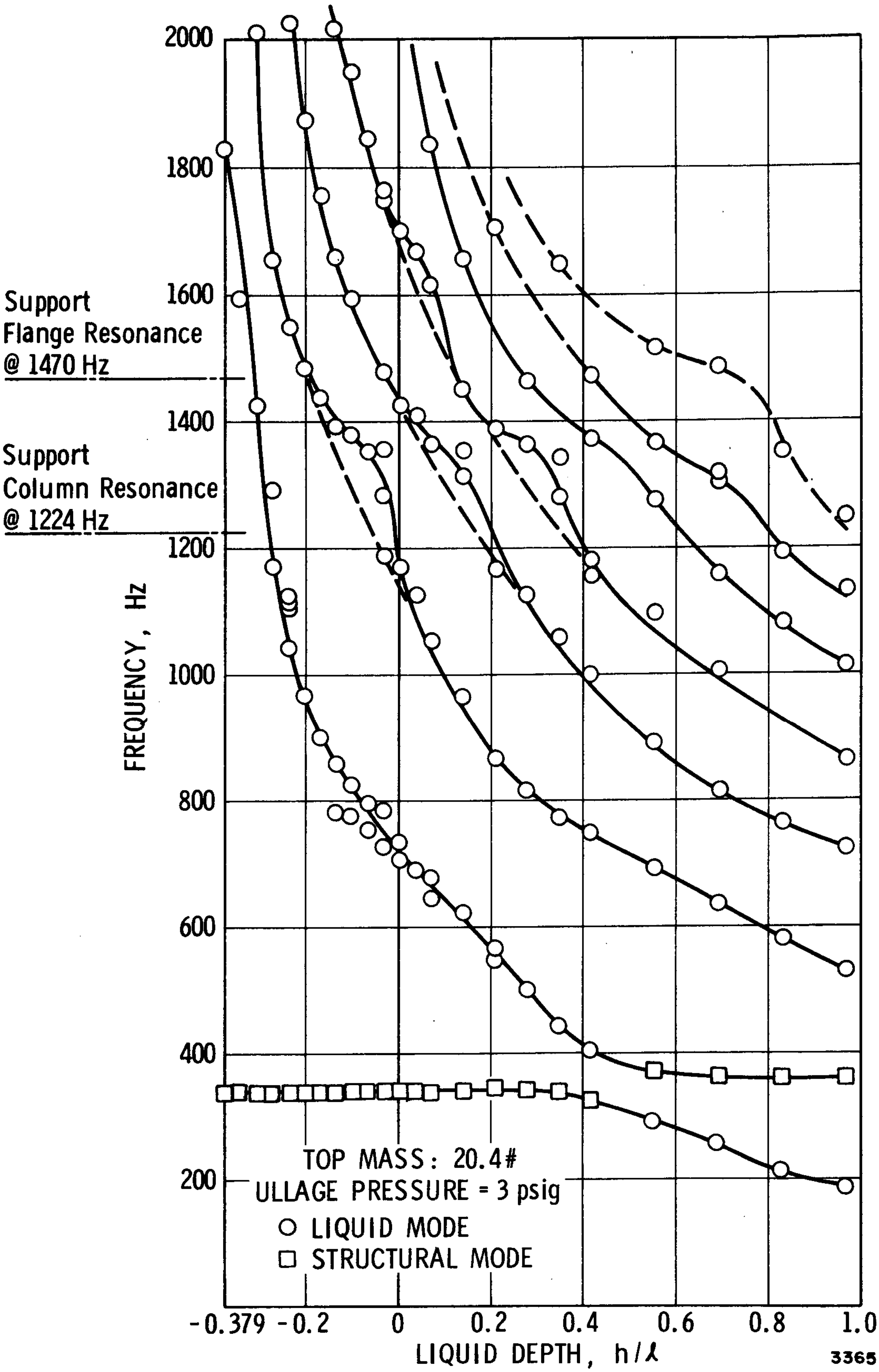

Figure 32. Natural Frequencies for Cylindrical Tank with Hemispherical Bulkhead-Stiffener Rings Configuration

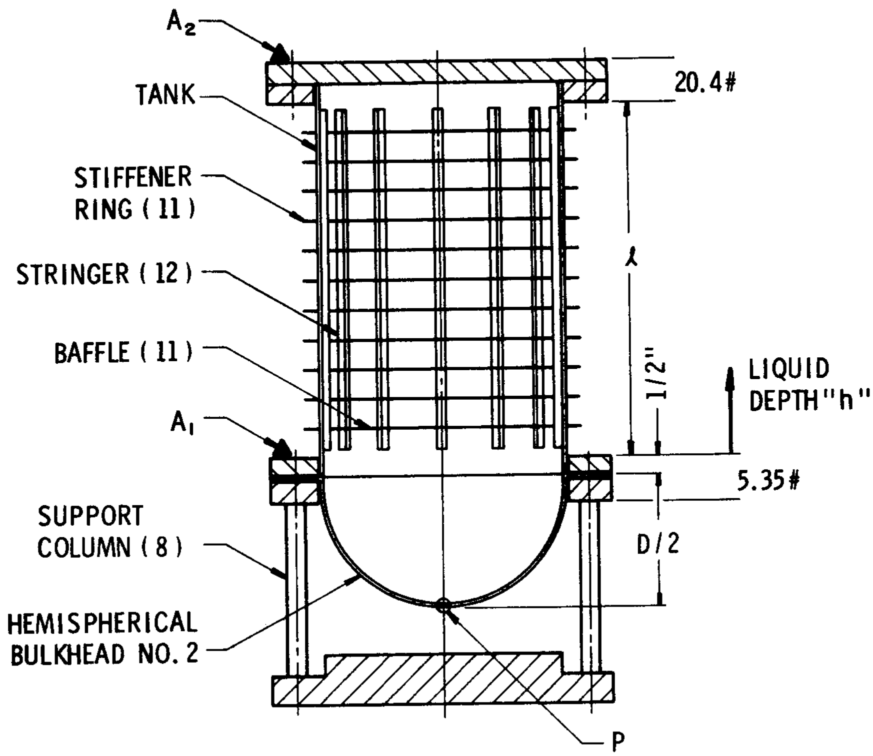

Structural Element	Effective Length (λ) (in.)	Inside Dia. (in.)	Wall Thickness (in.)	Material Density (#/in.^{3})	E x 10^6 psi
Tank	14.5	10.0	0.005	0.29	29
Bulkhead		D = 10.0	Fig. 3	0.098	10

Structural Element	Number Used On Tank	Material Density (#/in.^{3})	E x 10^6 psi	Dimensions (in.)	Location	Spacing (in.)
Stiffener Ring	11	0.098	10	10.0 I.D. 10.5 O.D. 0.032 Thick	Symmetrical about midspan	1.24
Stringer	12	0.098	10	0.125 x 0.125 x 14.0	Symmetrical about midspan	Equally spaced on inner circumference
Baffle	11	0.306	16	8.25 I.D. 9.68 O.D. 0.0125 Thick	Symmetrical about midspan	1.25

3366

Figure 33. Cylindrical Tank with Hemispherical Bulkhead-Stiffener Rings, Stringers, and Baffles Configuration

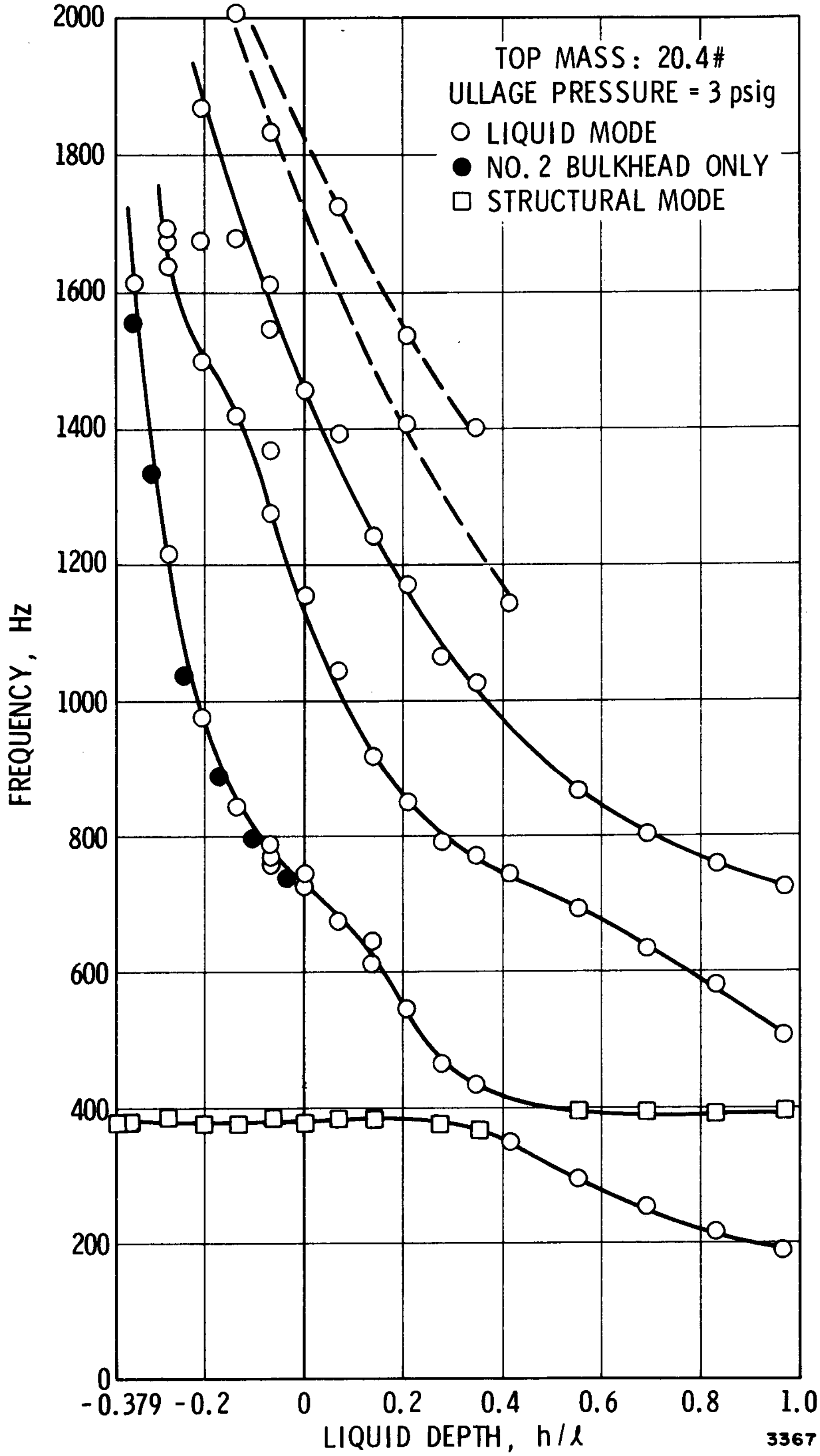

Figure 34. Natural Frequencies for Cylindrical Tank with Hemispherical Bulkhead-Stiffener Rings, Stringers, and Baffles Configuration

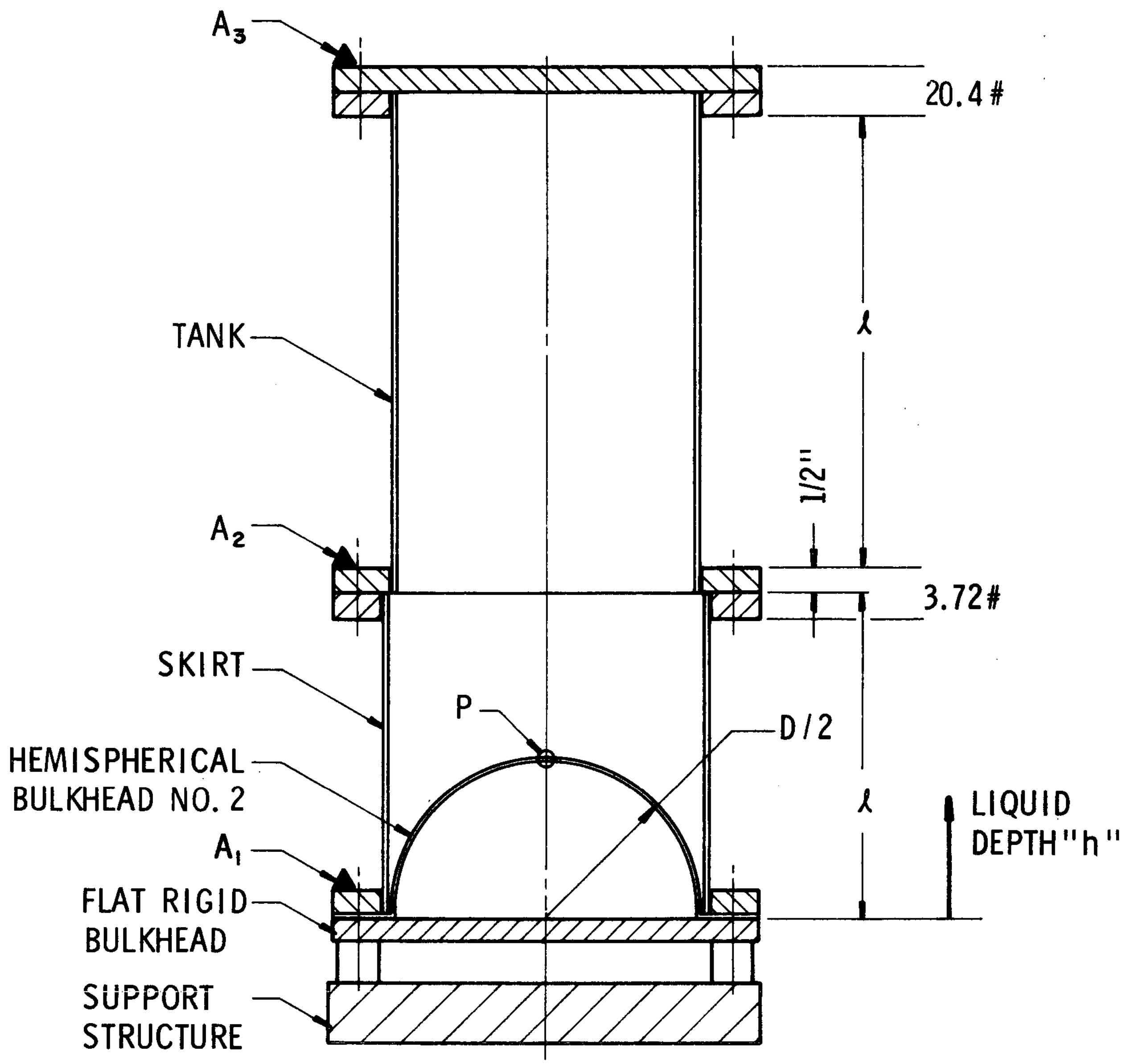

Structrual Element	Effective Length (ℓ) (in.)	Inside Dia. (in.)	Wall Thickness (in.)	Material Density (#/in^3)	E x 10^6 psi
Tank Skirt	14.5 7.5	10.0 10.3	0.005 0.025	0.29 0.098	29 10
Bulkhead		D = 10.0	Fig. 3	0.098	10

3368

Figure 35. Cylindrical Tanks with Inverted Hemispherical Bulkhead

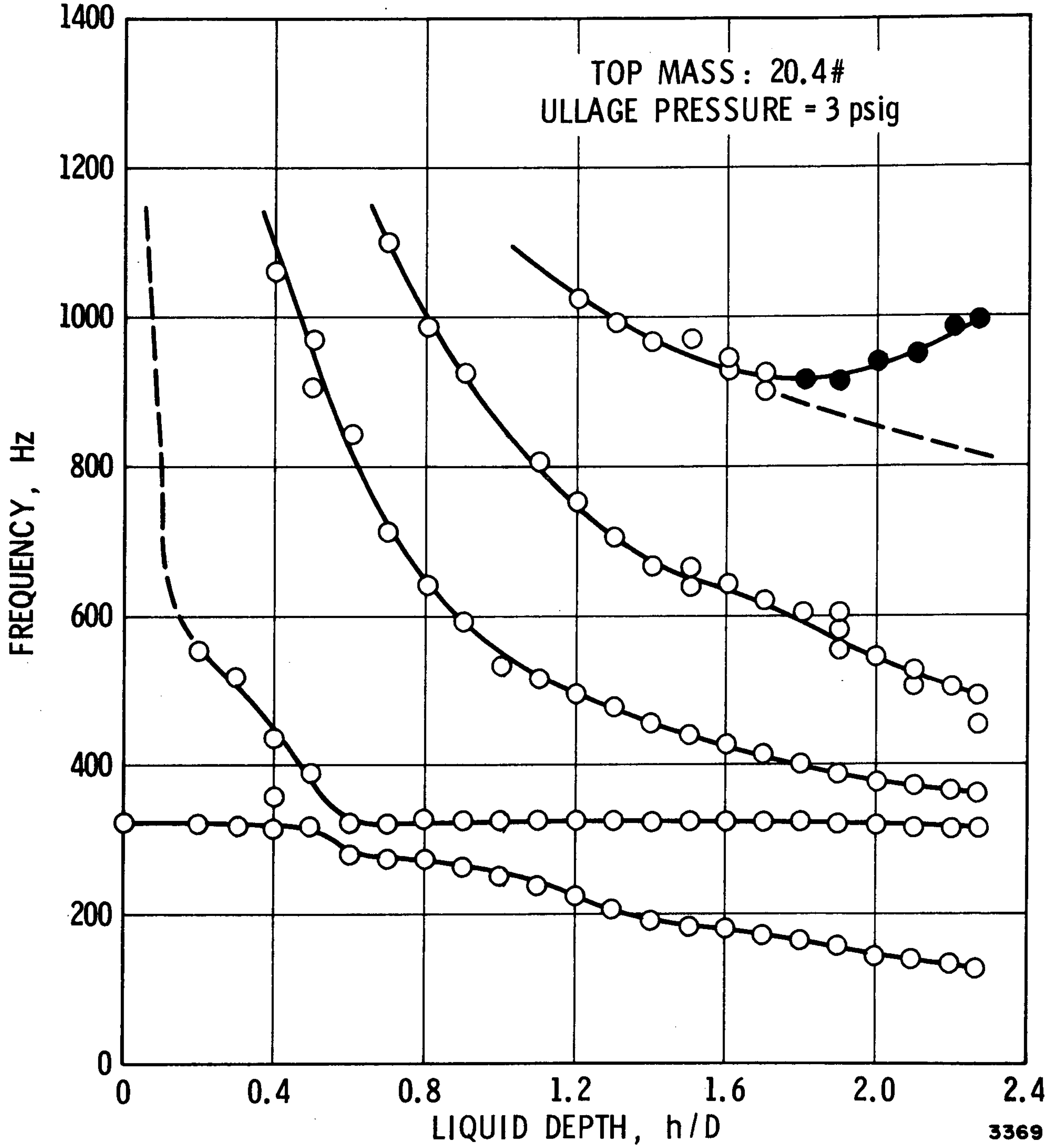

Figure 36. Natural Frequencies for Cylindrical Tank with Inverted Hemispherical Bulkhead

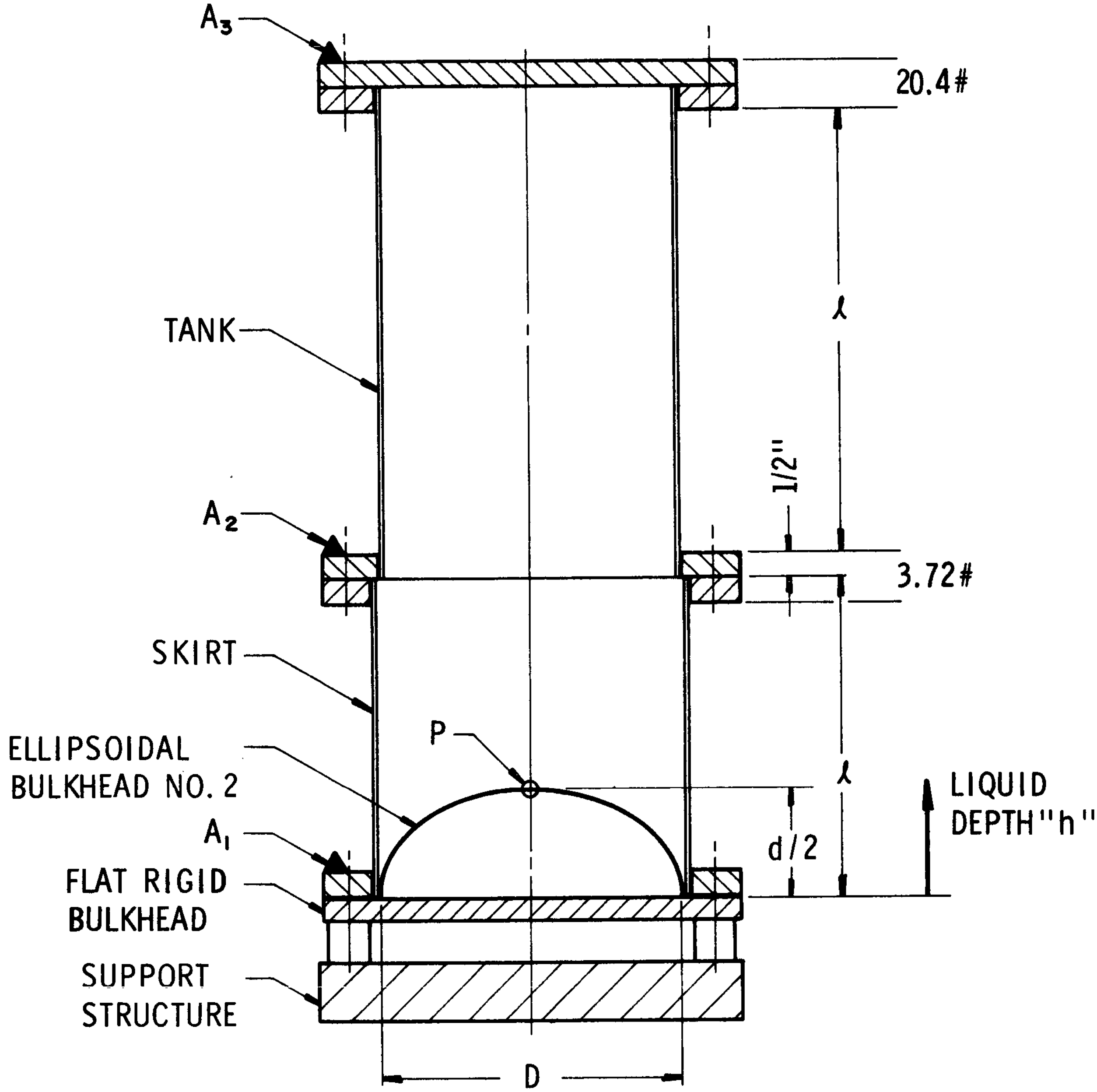

Structural Element	Effective Length (ℓ) (in.)	Inside Dia. (in.)	Wall Thickness (in.)	Material Density (#/in.^{3})	E x 10^6 psi
Tank	14.5	10.0	0.005	0.29	29
Skirt	7.5	10.3	0.025	0.098	10
Bulkhead		D = 10.0 d = 7.07	Fig. 4	0.098	10

3370

Figure 37. Cylindrical Tanks with Inverted Ellipsoidal Bulkhead

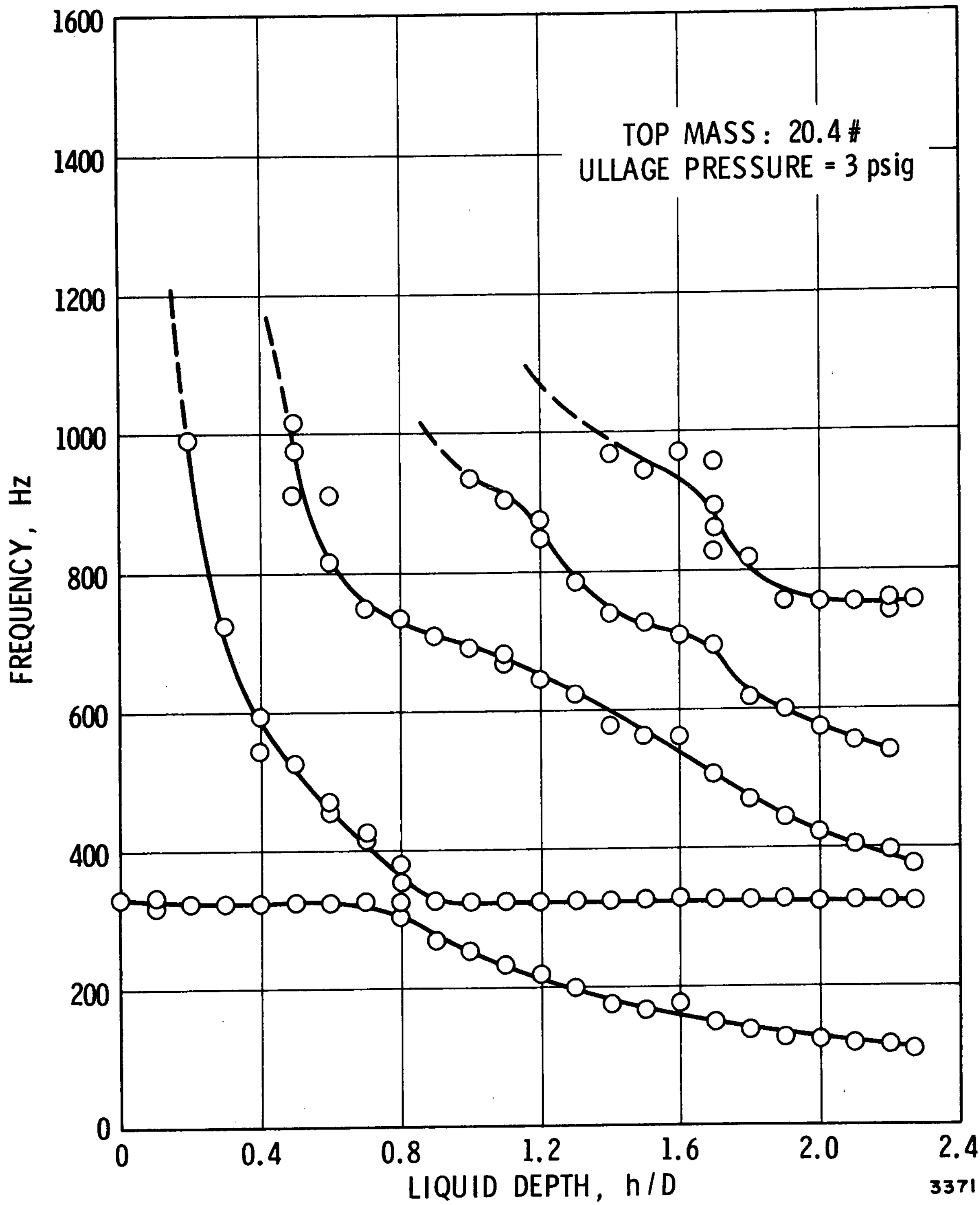

Figure 38. Natural Frequencies for Cylindrical Tanks with Inverted Ellipsoidal Bulkhead

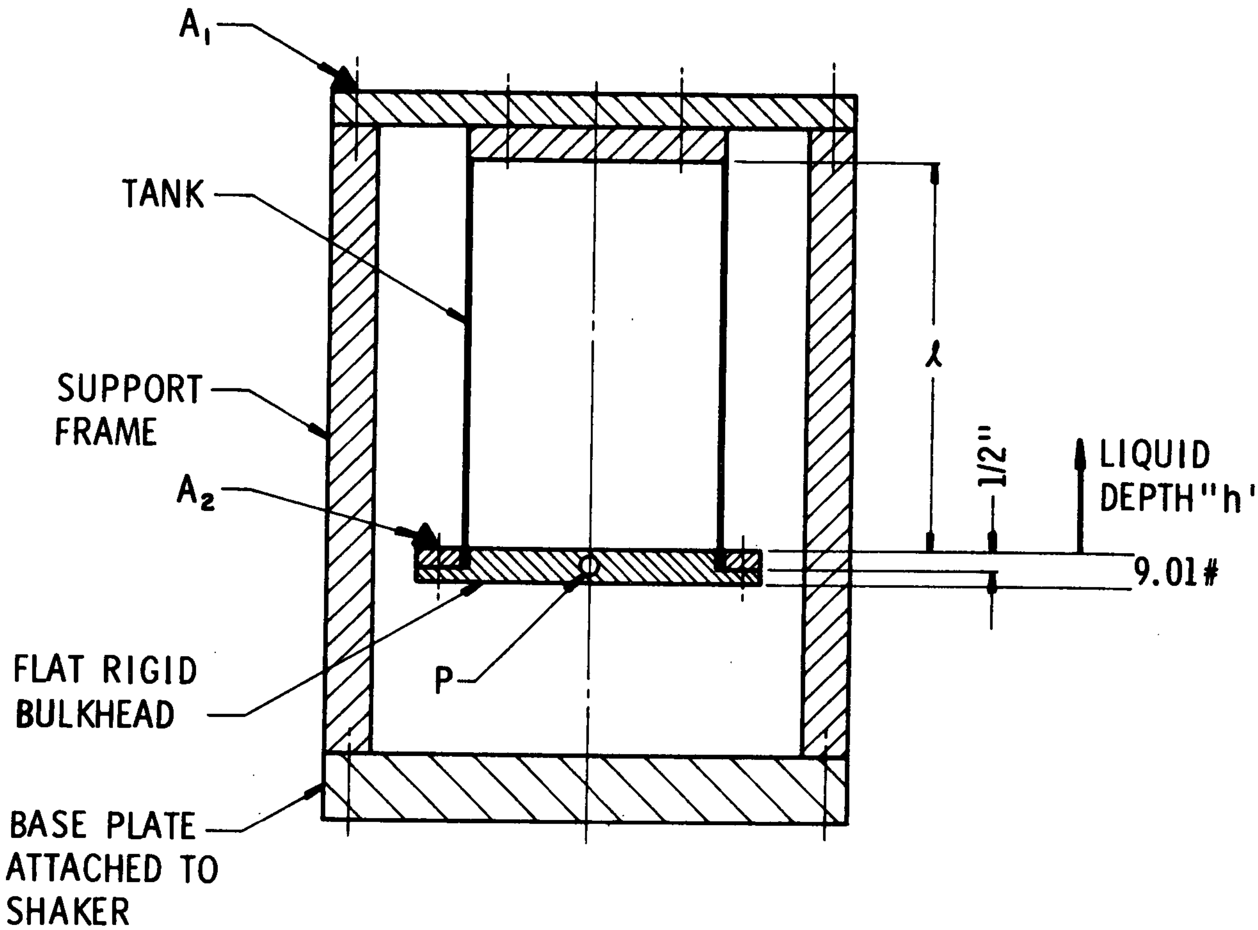

Structural Element	Effective Length (λ) (in.)	Inside Dia. (in.)	Wall Thickness (in.)	Material Density (#/in.^{3})	E x 10^6 psi
Tank	14.5	10.0	0.005	0.29	29

3372

Figure 39. Cylinder with Flat Rigid Bottom and Top Support

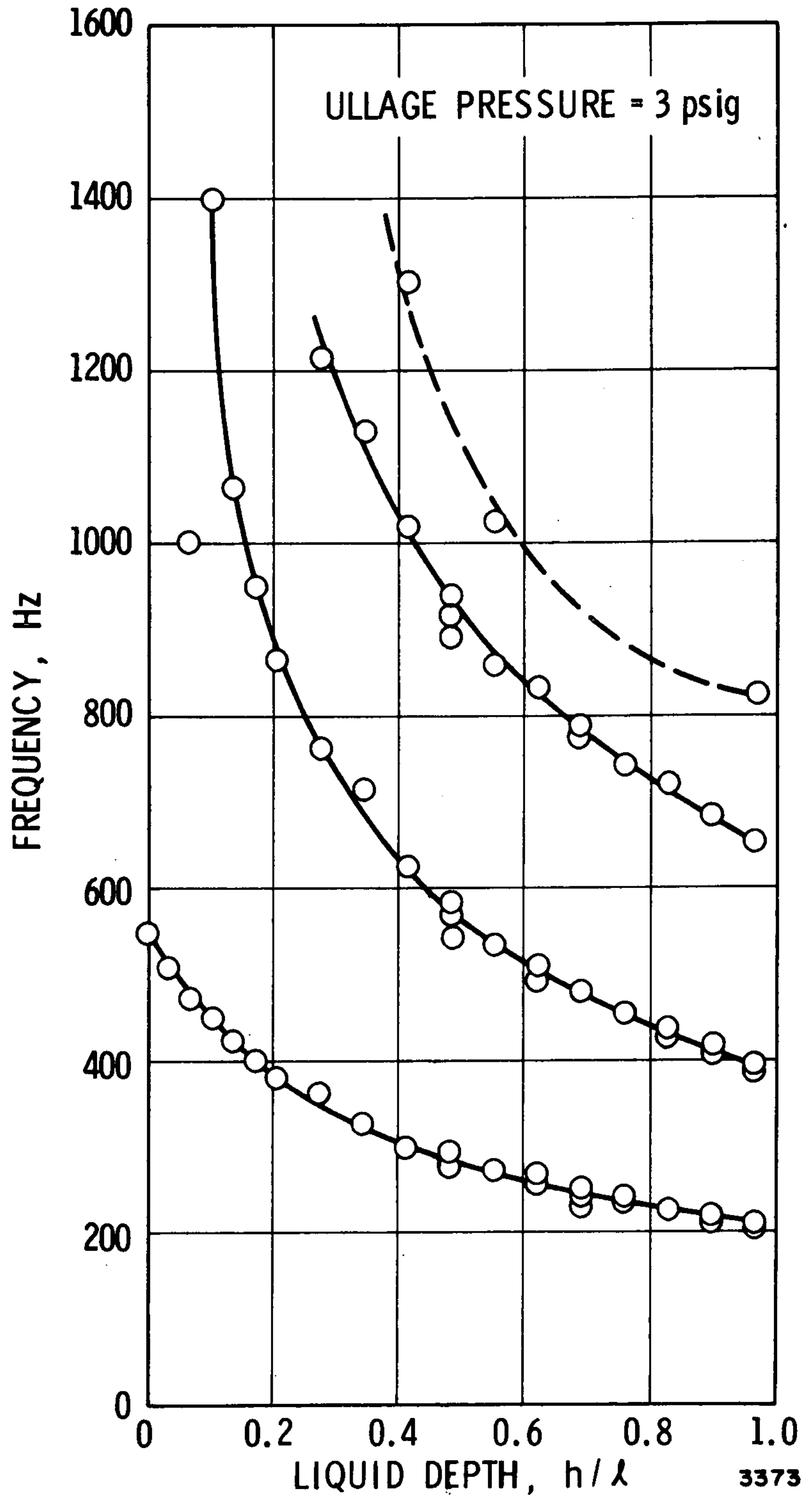

Figure 40. Natural Frequencies for Cylinder with Flat Rigid Bottom and Top Support

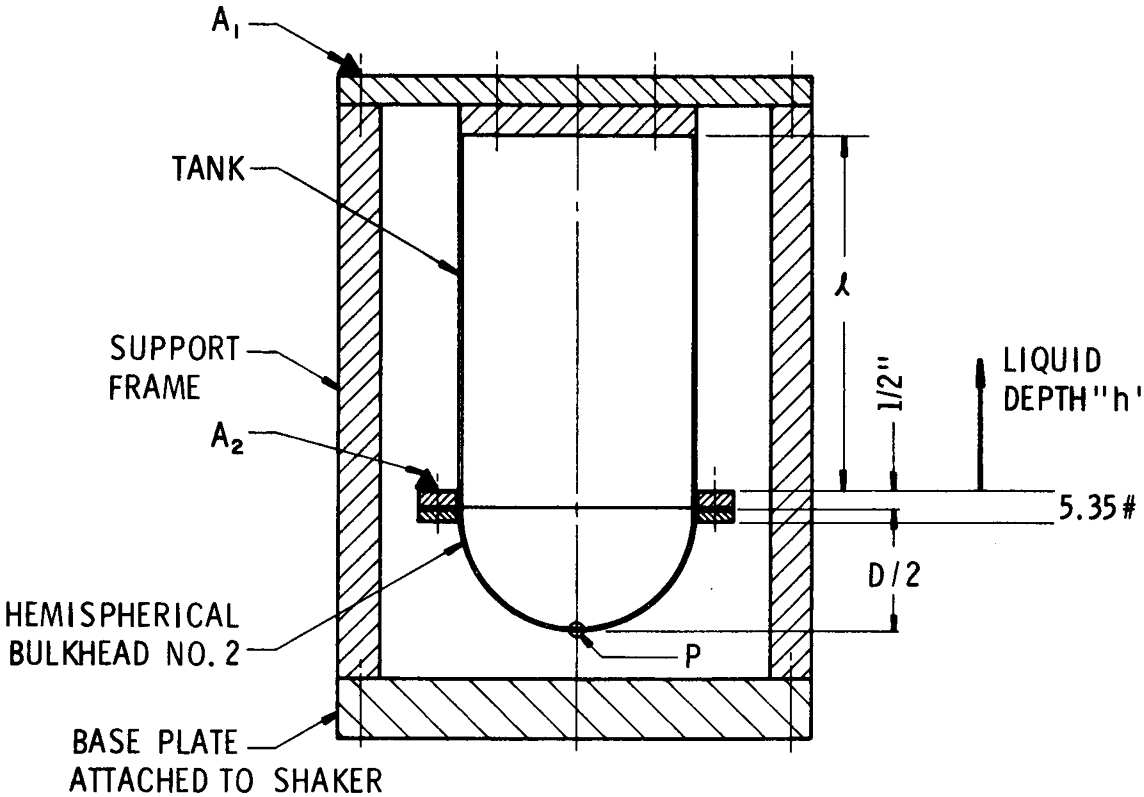

Structural Element	Effective Length (ℓ) (in.)	Inside Dia. (in.)	Wall Thickness (in.)	Material Density (#/in.^{3})	E x 10^6 psi
Tank	14.5	10.0	0.005	0.29	29
Bulkhead		D = 10.0	Fig. 3	0.098	10

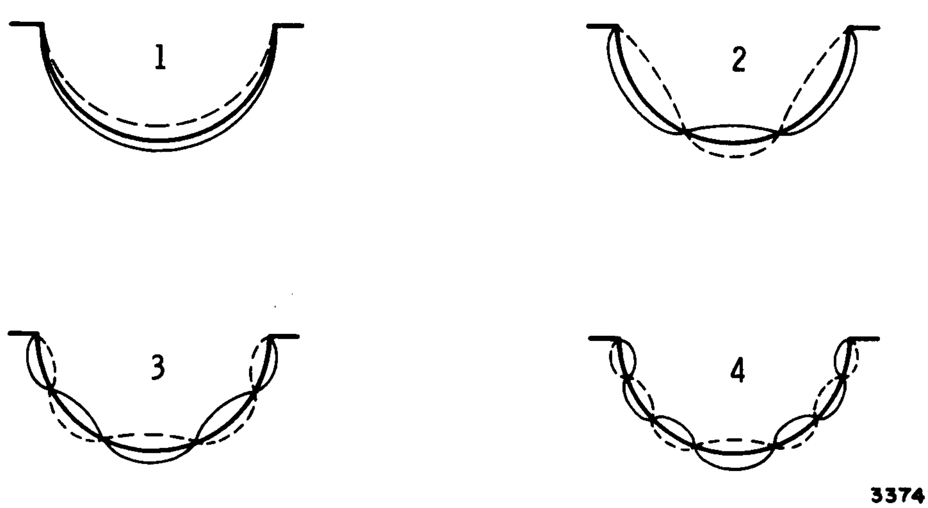

Figure 41. Cylinder with Hemispherical Bulkhead and Top Support

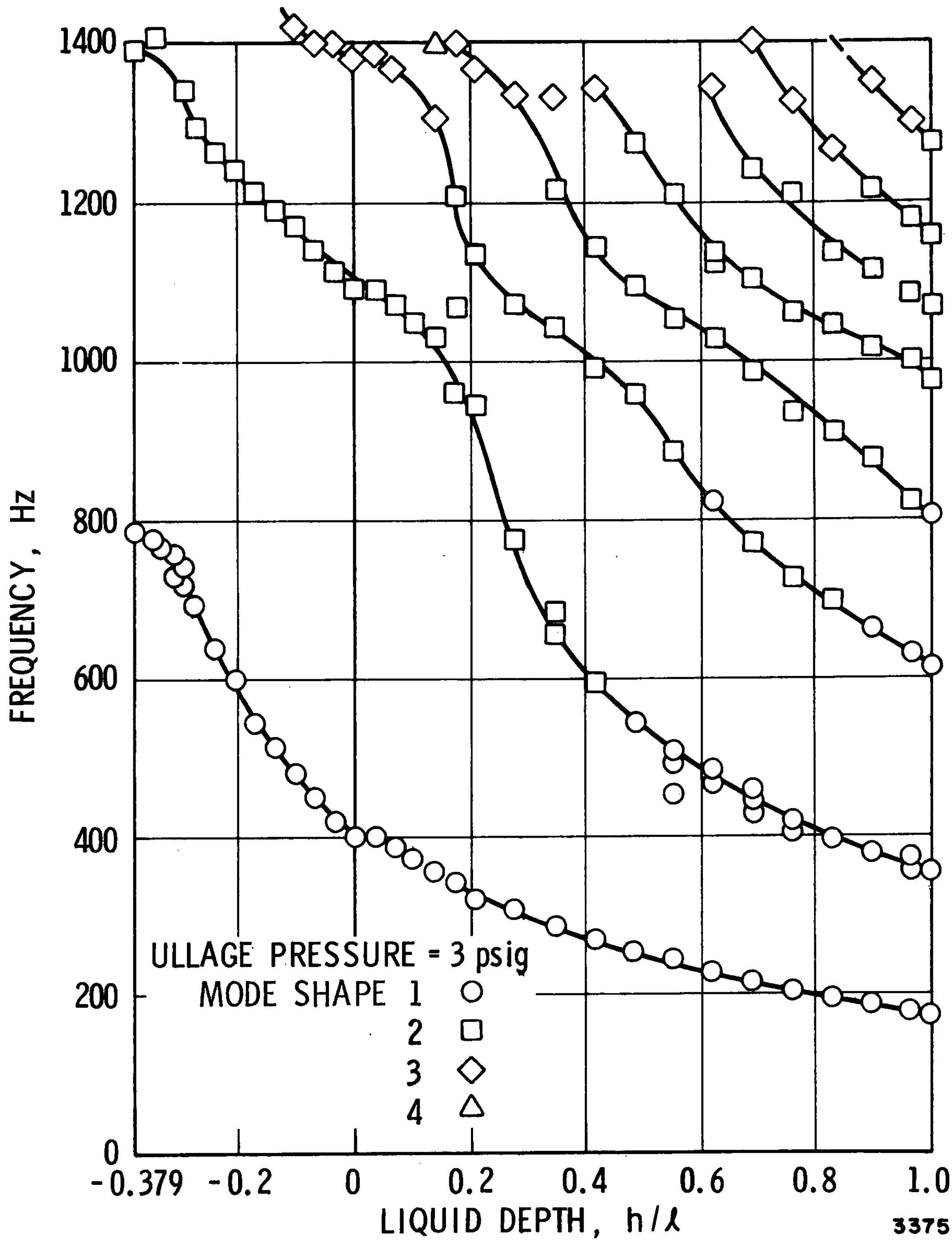

Figure 42. Natural Frequencies for Hemispherical Bulkhead and Top Support